High Resolution Seismic Reflection Survey to Image the Top and Bottom of a Shallow Clay Layer at the Memphis Defense Depot, Memphis, Tennessee

by

Richard D. Miller
Jianghai Xia
Jeffrey W. Deane
Joe M. Anderson
David R. Laflen
Patricia M. Acker
Mary C. Brohammer

of the
Kansas Geological Survey
The University of Kansas
Lawrence, Kansas

Introduction

Fluid movement across the surface or subsurface boundaries of the Defense Depot in Memphis Tennessee (DDMT) is of interest to the US Army Corps. The Huntsville Office of the Corps of Engineers, through the US Army Corps Waterways Experiment Station initiated a shallow seismic reflection survey in an attempt to determine lateral continuity and surface topography of a water table perching clay unit previous encountered during evaluation drilling. A small feasibility study was undertaken to determine the potential of the technique (Miller, 1993). Preliminary analysis suggested it should be possible to imagine at least the top of the clay with the proper equipment. Considering the finding of the feasibility study and with the alternative being grid drilling, approval was granted for a 1200 ft CDP feasibility line between guard shack #15 (located in the northwest corner of the main installation) and the west fence.

The high resolution seismic survey was originally proposed to consist of a single line approximately 2500 ft. The proposed primary targets were the top and bottom of a clay layer at between 80 and 150 ft overlying the Memphis sand (based on cross-section derived from old drill records) and any potentially hydrologically significant layers between the ground surface and the base of the Memphis sand. The primary goal was to determine the overall thickness of the clay and determine if it represents a non-permeable interface between the ground surface and the Memphis sand. Lateral discontinuity of the clay from either erosion or faults/joints were of particular interest.

The survey was conducted on January 24 and 25 of 1994. The project consisted of several walkaway noise tests and a 160 shotpoint, nominal 24 fold CDP line. The surface conditions required the opening of a 3 ft wide 1.5 ft deep trench across the gravel storage yard for the receivers and a secondary trench 2/3 ft deep and 1 ft wide for the source. The source was detonated and the receiver were planted into a clay cap that underlay the gravel surface cover over the entire site west of the railroad spur (Figure 1). The ground surface was damp and with several small pools of water in the geophone trench on the first day of shooting. The walkaways and the first 60 shotpoints of data were collected on the 24, with the remaining 100 shotpoints of the CDP line collected on the 25. The night of the 24 a significant rainfall was recorded filling the geophone and source trench. The powerline induced noise (60 Hz, 120 Hz, 180 Hz, etc.) was visible on recorded data on the 24th, but due to an increase in the conductivity of the soils after the rain, the powerline noise was overwhelming

on the 25. The increase in recorded powerline noise was the primary factor that hampered the overall quality of the recorded data.

Data Acquisition

Data for this study were acquired on a 48-channel EG&G Geometrics 2401x seismograph. The seismograph amplifies, filters (analog), digitizes the analog signal into a 15-bit word, and stores the digital information in a demultiplexed format. Analog filters have an 18 dB/octave rolloff from the selected -3 dB points. The 1/2 ms sampling interval resulted in a 2000 Hz sampling frequency for a record length of 500 msec and a 1000 Hz Nyquist frequency. A 250 Hz high-cut filter with a 24 dB/octave rolloff acted as an anti-alias filter and to reduce wind noise and higher modes of 60 Hz power line noise. The Geometrics 2401x is a floating point seismograph. The dynamic range of the seismograph was more than adequate to record high-quality reflection information at this site in the presence of source-generated and cultural noise.

Walkaway data were acquired with a variety of field parameters, offsets, and source energy in an attempt to optimize the production data (Figures 1 through 10). The sources for the testing included the 8- and 12-gauge auger gun (Healey et al., 1991). The receivers for the entire study were Mark Products L-28E 40 Hz geophones wired in series with three geophones per string. The station spacing for the walkaways was 4 ft. The resulting walkaway spreads possessed 96 traces with offsets ranging from 8 ft to 196 ft (source locations off both ends of the line were occupied).

Direct wave, refractions, ground roll, reflections, and air-coupled wave can all be identified on the walkaway data (Figures 1 through 10). Reflections can be interpreted best on most data recorded with close offsets (i.e. <200 ft). All aspects of the testing were necessary to first determine if it was feasible to proceed with and secondly to properly fine-tune the acquisition parameters and equipment for the CDP portion of the study.

The production portion of the survey involved 160 shotpoints along a single east/west line roughly parallel to the north fence with 8 ft station spacings. The source for the CDP data was the 8-gauge auger gun. The three geophones were placed in a 3 ft in-line array to help attenuate source-generated air coupled wave. The seismograph was configured to focus on reflections from the upper 250 msec with average velocities from 1200 to 6000 ft/sec. The pre-amplified spectra was shaped with 50 Hz analog low-cut filters, in an attempt to enhancing the higher

2

frequency components of the recorded energy. This emphasis on pushing the high side of the spectra was necessary to separate the reflections from the top and bottom of the 80 ft clay.

Data Processing

Data processing was done on an Intel 80486-based microcomputer using *Eavesdropper*, a set of commercially available algorithms. The processing flow was similar to those used in petroleum exploration (Table 1). The main distinctions relate to the conservative use and application of correlation statics, precision required during velocity and spectral analysis, extra care during muting operations, and lack of deconvolution.

For most basic shallow, high-resolution seismic reflection data the processing steps/operations are a simple scaling down of established petroleum-based processing techniques and methods. However, processes such as deconvolution have basic assumptions (Yilmaz, 1987) that are violated by most shallow data sets. Migration is another operation that, due to non-conventional scaling (vertical and/or horizontal), many times may appear to be necessary when in actuality geometric distortion may be simple scale exaggeration (Black et al., 1993). Processing/processes used on data for this report has/have been carefully executed with no *a priori* assumptions and with care not to create anything during a processing operation that was not present before.

To reduce the effects of the powerline noise and to attenuate ground roll, air-coupled wave, and refracted arrivals f-k filtering and digital bandreject filtering was evaluated (Figures 13 through 15). F-k filtering (also referred to as velocity filtering, slope filtering, pie filtering) successfully removed linear arrivals and effectively narrowed the bandwidth of the reflection information. The narrowing of the bandwidth resulted in the ringy appearance of the reflection wavelets. The narrowing of the wavelets was so dramatic that the reflections interpreted from the top and bottom of the clay began to interfere.

Results

Unequivocal identification of reflection energy on field files is essential for accurate interpretation of CDP stacked sections. A few of the digitally filtered field files acquired during the production portion of the survey have reflection events identifiable between 70 and 150 msec. The reflections have a dominant frequency of

approximately 80 Hz and an apparent NMO velocity of approximately 2750 ft/sec. These would result in an approximate depth to the reflector of between 100 and 180 ft. The signal-to-noise ratio on the raw field files is sufficient to confidently identify reflections on most files on the west end of the line, however, the 60 Hz noise (180 Hz) is sufficiently strong most longer-offset files are saturated with noise.

Analysis of processed field files improves confidence in interpretations of CDP-stacked sections. Digital filtering, first arrival muting, appropriate trace balancing, bad trace editing, and correlation statics were key processes in improving the pre-stack appearance of coherent events interpretable on raw field files (Figures 11, 17-19). The coherent events identifiable on some of the filtered files possess an arrival pattern consistent with the classic hyperbolic moveout of a reflection (Figure 16). These interpreted reflection arrivals allows significant confidence in interpreting the CDP stacked section. It is still prudent to practice care and a conservative approach to interpretations of coherent energy on stacked data.

Coherent events can be interpreted across all the CDP stacked sections (Figures 20 through 23). The stacked sections possess nominal 24 CDP fold as a result of the 48-channel recording system and the recording geometry. The fold drop near the ends of the lines inhibits high confidence in interpretations within 20 CDP of the line ends. There are two correlatable events between 60 and msec. The extreme curvature of most of the events and the lack of consistent source wavelet characteristics minimized accurate correlation of events from line to line.

The near-surface conditions were poor. The gravel fill overlying a clay cap of unknown thickness represents a less than conducive environment for the collection of high quality seismic data. The near-surface material changed 2/3 of the way across the line from gravel pack over clay to railroad bed and grass over clay fill on the east end. Even with these poor conditions the technique showed significant promise during testing and production the first day. The dominant frequency of body wave energy and the narrow band nature (very cyclic, ringy with attempts to shape the spectrum) of most arrivals on field files is consistent with this very difficult near-surface.

The dominant frequency of most recorded reflection energy is between 50 and 100 Hz. The stacking velocity ranged from 2000 to 3500 ft/sec. The subsurface geology interpreted from borehole data should be very conducive to shallow reflection techniques. The existing borehole data suggest a clay layer about 60 to 80 ft thick and 80 ft deep on the west end of the seismic line. The top of the water table is

4

interpreted to follow the contours of the clay and is about 5 to 10 ft above the clay surface. A second borehole near the east end of the line encounter the clay layer at over 140 ft of depth with the water table directly above the clay. These conditions and subsurface geometries should represent an ideal application for the technique. The stacked section provide marginal resolution potential but excellent coherence over the west half of the line. Severe muting and advanced pre-stack processing (i.e. f-k filtering, deconvolution, etc.) did little to enhance the interpretation on the west and nothing to improve the confidence in interpreting data on the east.

The CDP stacked section possesses two interpretable reflection (Figure 22). The shallowest reflection (80 msec) is approximately 100 ft deep (based on NMO velocities). The second reflection (115 msec) is approximately 160 ft deep (again based on NMO velocities. The apparent time structure of the events is somewhat dictated by near-surface irregularities in velocity. Therefore, the apparent shallowing of the 80 msec event from west to east is probably accurate however the synclinal feature between CDP 330 and 400 is probably the result of static irregularities. The evidence that supports this conclusion is the way the two independent events mirror each other over this spatial distance. From CDP 400 to 500 the increased powerline noise is evident. Interpreting reflections in this window would be speculative. The subtle presence of reflections could be interpreted. The reflection seem to suggest the top of clay actually gets shallower and the clay thickens to the east up to CDP 400, where it seems to drastically thin.

The thinning does not seem to result in a pinch-out. Even with the poor data quality, a case could be made that the clay thins but does not pinch-out. Verification of this would be possible with drilling. If the conditions on the first day of data acquisition could be maintained it would be feasible to extend the higher quality coverage to the guard shack.

The brute stack section with the first arrival still present can be used to remove at least some of the near-surface velocity irregularities (Figure 23). The arrival present at about 40 msec across the line is a shallow refraction. By flattening this event (which makes some assumptions about its origin) some of the near surface static should be removed and a more accurate interpretation made. It is clear from this shallow event about a 10 msec pull-up in time is present on the east end of the line.

Conclusions

The data acquisition conditions were difficult at best. The high levels of cultural noise and fill material covering the entire site had a detrimental effect on the overall data quality. The heavily traveled road, power lines, noise from machinery, surface obstructions, and fill material negatively effective the resolution potential of data collected at this site. Even with these conditions interpretable results are possible at this site. The statics are a problem but with uphole surveys conducted in any wells installed and refraction statics a confident tie to the boreholes should be possible. It is our option that the clay layer thins to less than 30 ft beneath CDP 500 but does not pinch-out.

Recommendations

Boreholes and velocity check shots would be a minimum at this site. A bore hole at CDP 230 and CDP 390 with associated uphole surveys would allow a more confident interpretation of the seismic data. With the incorporation of this data both the validity of the CDP data and its associated interpretation could be verified. If the borehole and velocity complement the CDP stacked section a second line that starts near CDP 330 and extends beyond the guard shack on the east when conditions are better (i.e. when it is not raining and the ground is drier) should resolve the depression suggested on the eastern end of this line.

References

Black, R.A., D.W. Steeples, and R.D. Miller, 1993, The utility of migration on shallow seismic reflection data: *Geophysics*, v. 59, n. 3, p. 402-410.

Goforth, T., and C. Hayward, 1992, Seismic reflection investigations of a bedrock surface buried under alluvium: *Geophysics*, v. 57, n. 9, p. 1217-1227.

Healey, J., J. Anderson, R.D. Miller, D. Keiswetter, D.W. Steeples, and B. Bennett, 1991, Improved shallow seismic-reflection source: building a better Buffalo [Exp. Abs.]: Soc. Explor. Geophys. v. 1, p. 588-591.

Miller, R.D., D.W. Steeples, and P.B. Myers, 1990, Shallow seismic-reflection survey across the Meers fault, Oklahoma: *Geological Society of America Bulletin*, v. 102, p. 18-25.

Miller, R.D., D.W. Steeples, R. Hill, and B. Gaddis, 1990, Identifying intra-alluvial and bedrock structures shallower than 30 meters using seismic-reflection techniques: Soc. Explor. Geophys. volumes on Geotechnical and Environmental Geophysics, Stan Ward, ed., *Volume 3: Geotechnical*, p. 89-98.

Miller, R.D., and D.W. Steeples, 1986, Shallow structure from a seismic reflection profile across the Borah Peak, Idaho, fault scarp: *Geophysical Research Letters*, v. 13, p. 953-956.

Myers P.B., R.D. Miller, and D.W. Steeples, 1987, Shallow seismic reflection profile of the Meers fault, Comanche County, Oklahoma: *Geophysical Research Letters*, v. 14, p. 749-752.

Steeples, D.W., and R.D. Miller, 1990, Seismic-reflection methods applied to engineering, environmental, and ground-water problems: Soc. Explor. Geophys. volumes on Geotechnical and Environmental Geophysics, Stan Ward, ed., *Volume 1: Review and Tutorial*, p. 1-30.

Steeples, D.W., R.D. Miller, and R.W. Knapp, 1987, Downhole .50-caliber rifle–an advance in high-resolution seismic sources, [Exp. Abs.]; *in* Technical Program Abstracts and Biographies: Soc. Explor. Geophys. 57th Ann. Mtg., p. 76-78.

Treadway, J.A., D.W. Steeples and R.D. Miller, 1988, Shallow seismic study of a fault scarp near Borah Peak, Idaho: *Journal of Geophysical Research*, v. 93, no. B6, p. 6325-6337.

Yilmaz, O., 1987, Seismic data processing; S. M. Doherty, Ed.; *in* Series: Investigations in Geophysics, no. 2, Edwin B. Neitzel, Series Ed.: Soc. of Explor. Geophys., Tulsa, Oklahoma.

TABLE 1

Processing flow

format from SEG2 to KGSEGY

preliminary editing (automatic bad trace edit with 10 msec noise window)

trace balancing (150 msec window)

first arrival muting (detailed trace by trace mutes based on arrival identification)

surgical muting (removal of air coupled wave based on trace-by-trace arrival)

assign geometries (input source and receiver locations)

sort into CDPs (re-order traces in common midpoints)

velocity analysis (whole data set analysis on 100 ft/sec increments)

spectral analysis (frequency vs amplitude plots)

NMO correction (station dependent ranging from 2,250 to 3,500 ft/sec)

digital filtering (bandpass 40-80 200-275)

secondary editing (manual review and removal of bad or noisy traces)

CDP stack

amplitude normalization (AGC 50 msec with 20 msec delay)

display

Table 1. Processing flow for CDP stacked data. Parameters were determined by analysis for each prior step as well as through iterative analysis of particular operations.

FIGURE CAPTIONS

Figure 1   Two 96-channel walkaways recorded with low-cut filters out using the 12- and 8-gauge auger gun positioned off the west end of the spread. The pre-first arrival energy is from traffic on the east-west road approximately 150 ft from the line. Comparison of 100 (12-gauge auger gun) and 200 (8-gauge auger gun) shows the increase in recorded signal by the 8-gauge source. The very attenuative nature of this site is evident when refraction energy from the 8-gauge auger gun is difficult to identify beyond about 200 ft.

Figure 2   Two 96-channel walkaways recorded with low-cut filters set at 50 Hz using the 12 and 8-gauge auger gun positioned off the west end of the spread. The power line noise is extremely evident at offsets greater than about 150 ft. The reflection interpreted at about 80 msec is interfered with by both the groundroll and the power line noise to a point that the fit of the hyperbolic curve representative of the appropriate move out velocity is less than perfect.

Figure 3   Two 96-channel walkaways recorded with low-cut filters set at 100 Hz using the 12- and 8-gauge auger gun positioned off the west end of the spread. The powerline noise is sufficiently powerful at this filter setting so little can be interpreted except direct wave, ground roll, and air coupled wave.

Figure 4   Two 96-channel walkaways recorded with low-cut filters set at 200 Hz using the 12- and 8-gauge auger gun positioned off the west end of the spread. The data quality is extremely poor on these walkaways.

Figure 5   Two 96-channel walkaways recorded with low-cut filters set at 280 Hz using the 12- and 8-gauge auger gun positioned off the west end of the spread. No reflection data can be interpreted on these walkaways. The stronger energy 8-gauge source (204) has an obviously higher air-coupled wave.

Figure 6   This 96-channel walkaway with the 12-gauge auger gun has a analog low-cut of 100 Hz and an analog high-cut of 250 Hz. This test was to determine if narrow band recording would improve the signal-to-noise ratio of the recorded data. It is also clear from the walkaway that the powerline noise is saturating the dynamic range of the seismograph.

Figure 7   Two 96-channel walkaways recorded with low-cut filters out using the 8-gauge auger gun positioned off the west end (200) and off the east end (397) of the same spread. The sequence of reversed shots was designed to insure that source location was not contributing to any misidentification of arrivals. It is clear from the linear arrivals (refraction and direct wave) the near-surface on the east end of the line is slightly different than the west end. The proposed reflection event at 80 msec is still very evident.

Figure 8   Two 96-channel walkaways recorded with low-cut filters set at 50 Hz
using the 8-gauge auger gun positioned off the west end (201) and off the
east end (398) of the same spread.   The reflection is easiest to interpret on
the 50 Hz low-cut data.   When the source is off the east end the
direct/refracted arrival possess so little energy it is very difficult to
interpret.   The clean separation of the refraction and reflection slopes as
well as the divergence of the reflections from refractions is verification of
the reflection nature of the 80 msec event.   To insure that the 80 msec
event was not a misinterpreted refraction (which is the only other even
remote possibility) a refraction calculation was done on the event, and for
this event to be refraction it would be a layer 80 ft deep with a velocity of
5600 ft/sec and a time intercept of 350 msec.   The 80 msec event is not a
refraction.

Figure 9   Two 96-channel walkaways recorded with low-cut filters set at 100 Hz
with the 8-gauge auger gun positioned off the west end (202) and off the
east end (399) of the same spread.   The 100 Hz low-cut begins to narrow
the bandwidth and therefore the events, especially from the east end of
the line, where it is beginning to appear cyclic or ringy.   The powerline
noise is becoming a major problem at this filter setting.

Figure 10   Two 96-channel walkaways recorded with low-cut filters set at 280 Hz
with the 8-gauge auger gun positioned off the west end (204) and off the
east end (401) of the same spread.   The powerline noise is overpowering.

Figure 11   Digitally filtered field files from six places across the survey line.   Files A-
C show little effects of the power lines.   Files D-F are drastically altered by
the powerline noise.   The reflection events interpreted on walkaways are
present and prominent with the acquisition parameters and equipment
used to collected the production portion of the survey.   The 80 msec
reflection is very pronounce on the split spread field files having a classic
hyperbolic curvature.   The refraction arrival is clearly present on the files
a and b but the amplitude of the arrivals is not great enough to be
interpretable over the powerline noise on the other four files.

Figure 12   Increasing the digital band pass filter applied to Figure 11 decreased the
overall signal-to-noise ratio of the data.   The digital filter was raised from
40-80 Hz (low-cut ramp) on Figure 11 to 50-100 Hz (low-cut ramp) here.
This subtle increase is obvious and is suggestive of the very band limited
nature of the recorded reflection energy as a result of the recorded
powerline noise.

Figure 13   Band reject filtering was applied to remove as much of the 60, 120, 180,
and 240 Hz powerline noise as possible.   It is clear from this filtering
exercise that the seismograph's dynamic range was saturated with
powerline noise with little or no bits available for source generated
energy.

10

Figure 14   F-k filtering was applied to the six representative field files after band reject filtering in an attempt to remove the refracted and other high velocity arrivals. It is clear that little is present in the way of confident and consistent coherent arrivals that could be interpreted as reflections.

Figure 15   F-k filtering of the six representative field files after band reject filtering and refraction f-k filtering was applied to remove the air coupled wave. The results of this filtering exercise were less than encouraging in terms of improving upon the resolution potential of the simply digitally filtered field files.

Figure 16   Digitally filtered field files with a theoretical hyperbolic curve representing 2750 ft/sec and 69 msec vertically incident time on file (a) and 2500 ft/sec and 73 msec vertically incident time on file (b) superimposed on each file. The arrival pattern of the interpreted reflection is very consistent with expectation and the velocity and depth are appropriate for the geology and target as well.

Figure 17   The six representative digitally filtered field files have been gathered according to source-to-receiver offset distance. This allows improved coherence of the reflection arrivals and allows some qualitative appraisal of dip and static problems as well as consistency in recorded energy. Arrival recorded behind the source in some environments possess a degradation in over bandwidth and amplitude caused by the near-field effects of the source as it passes by when split-spread recording.

Figure 18   The representative six field files with groundroll muted out.

Figure 19   The representative six field files with groundroll, air-coupled wave, direct wave, refractions, and pre-first arrival noise muted.

Figure 20   Stacked section after complete muting, band reject filtering, band pass filtering, two f-k filters applied, corrected to vertical incidence, trace balanced, and stacked.

Figure 21   Stack section processed the same as Figure 20 without the air wave f-k filter.

Figure 22   Stacked section with complete muting, band pass filtering, corrected to vertical incidence, trace balanced, and stacked. This stacked section represents the most interpretable of the sections presented in this report. The dominant frequency of the stacked reflections is approximately 80 Hz. The divergence of the upper reflection from the lower reflection confirms the lower reflection is not a narrow band effect or a multiple of the upper event.

Figure 23   Stacked section with only ground roll muting, correction to vertical incidence, trace balanced, and stacked. This section allows the first arrival

to be interpreted and some idea of the amount and irregularity of the near-surface velocity.

Figure 24   Interpretation of Figure 22.

Figure 25   Figure 23 with the refraction interpreted for use as a reference for static removal on the interpretation in Figure 26. Assuming variations in the near-surface layer (probably the base of the clay fill) are present in the refraction arrival, by flattening the reflection beneath based on a true flat refraction, the resulting interpretation should be more accurate in comparison to depth determination from drilling. The resulting interpretation (given the previous assumption) should possess structures that are relatively unaltered by near-surface effects.

Figure 26   An approximate depth interpretation of the two reflecting events previously identified. The interpretation presented here has been time adjusted prior to depth conversion for static apparent in the stacked refraction. If the assumption made in the caption for Figure 25 are accurate, this should be a representative cross-section.

Figure 1
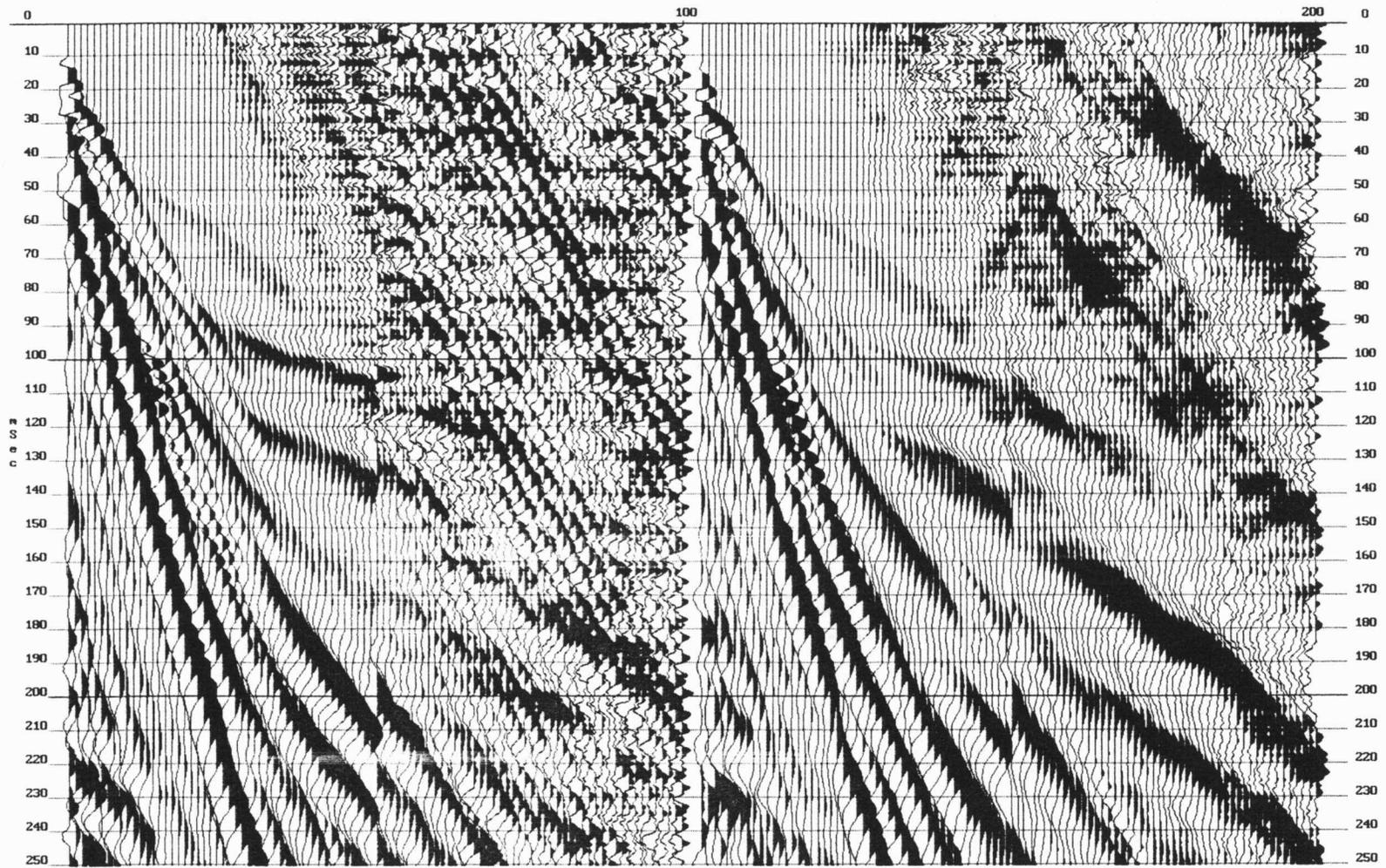
Figure 2
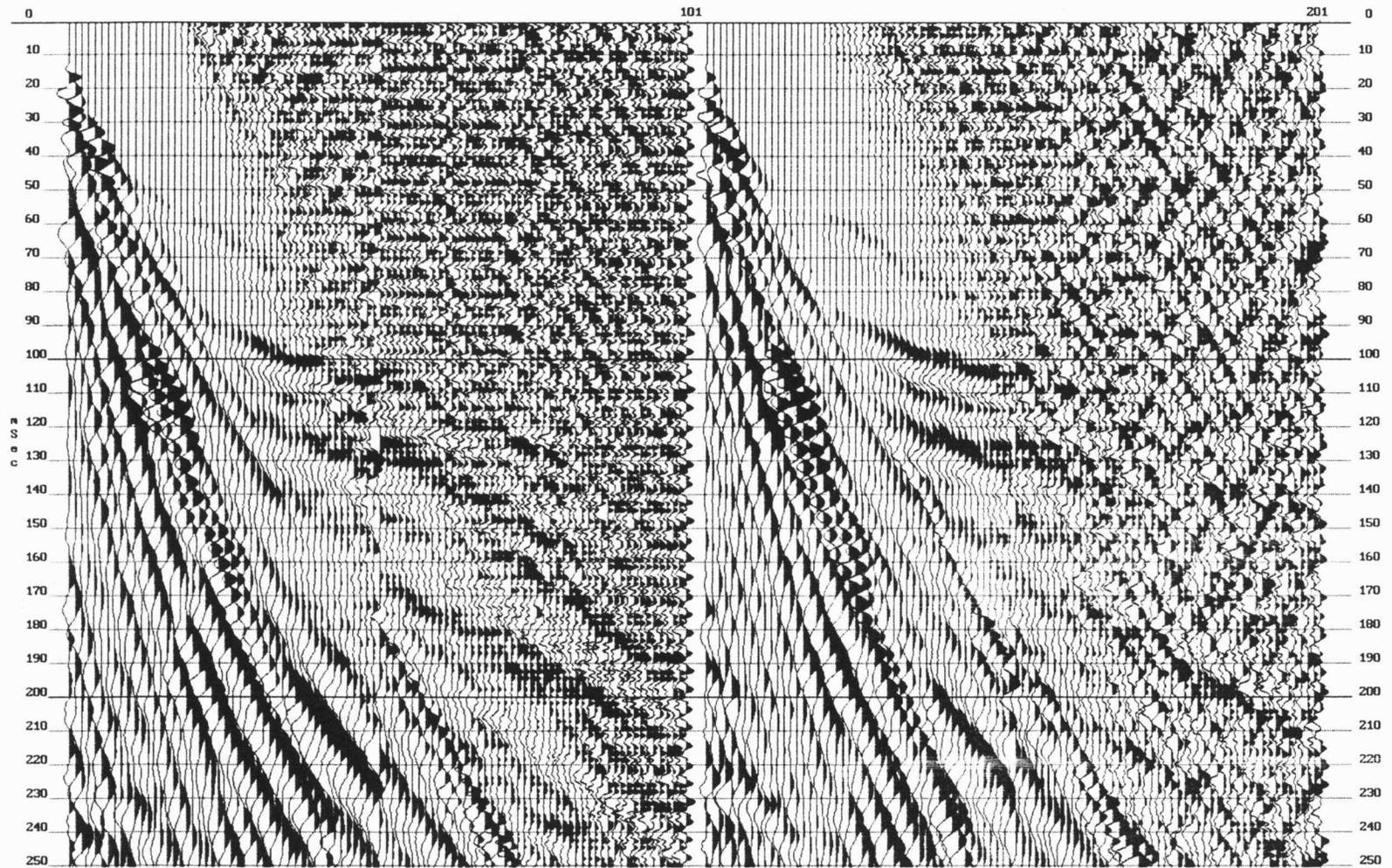
Figure 3
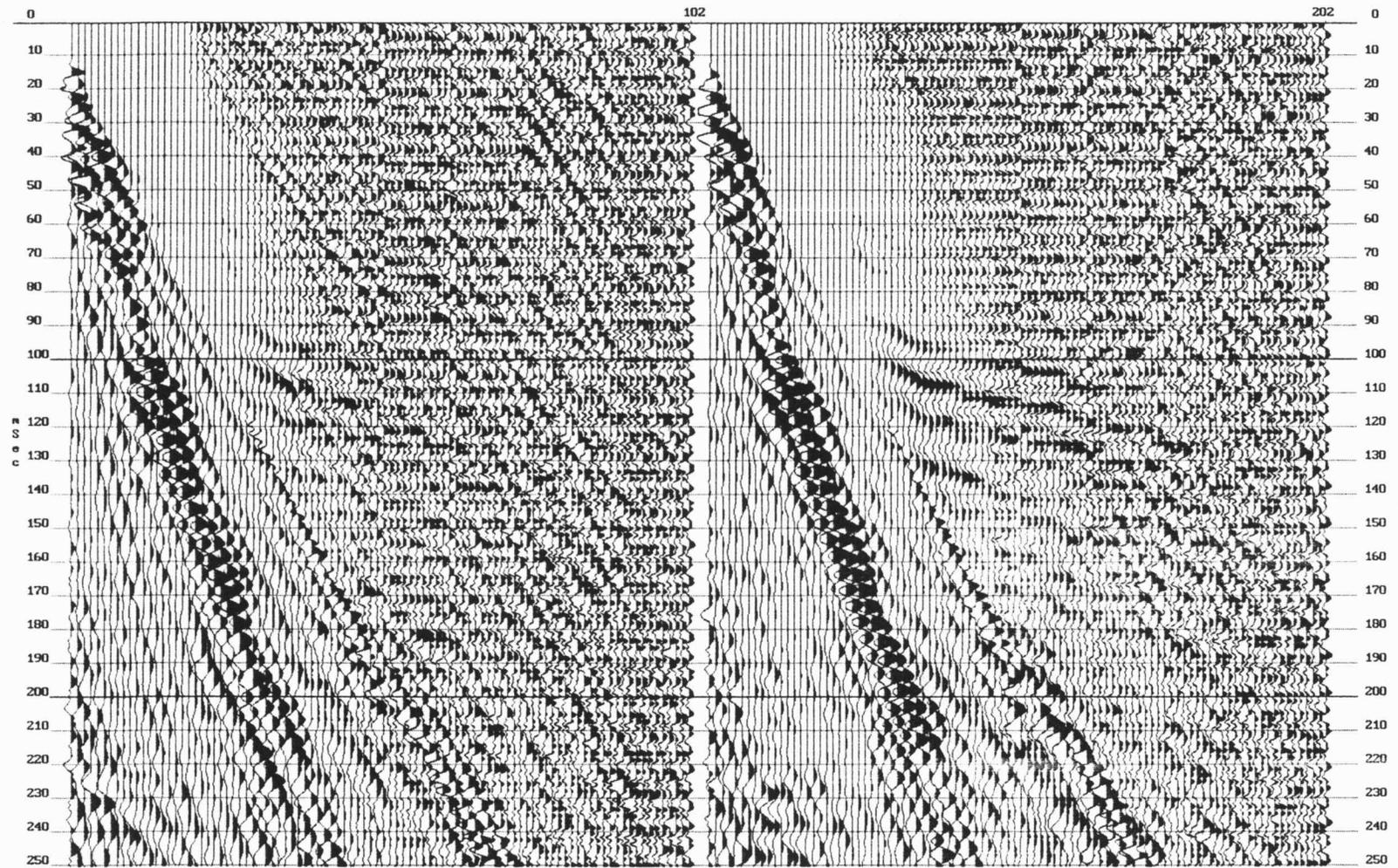
Figure 4
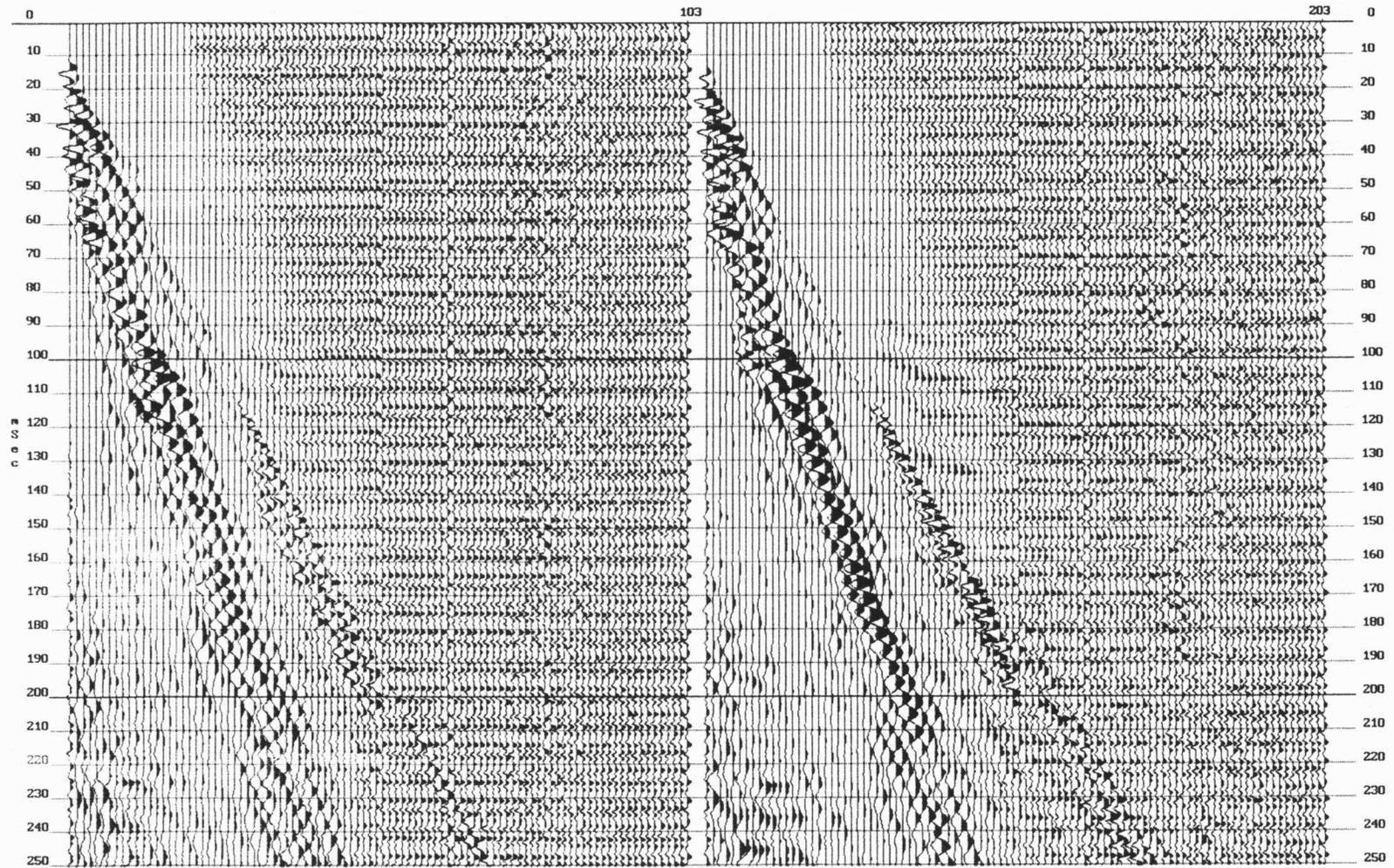
Figure 5
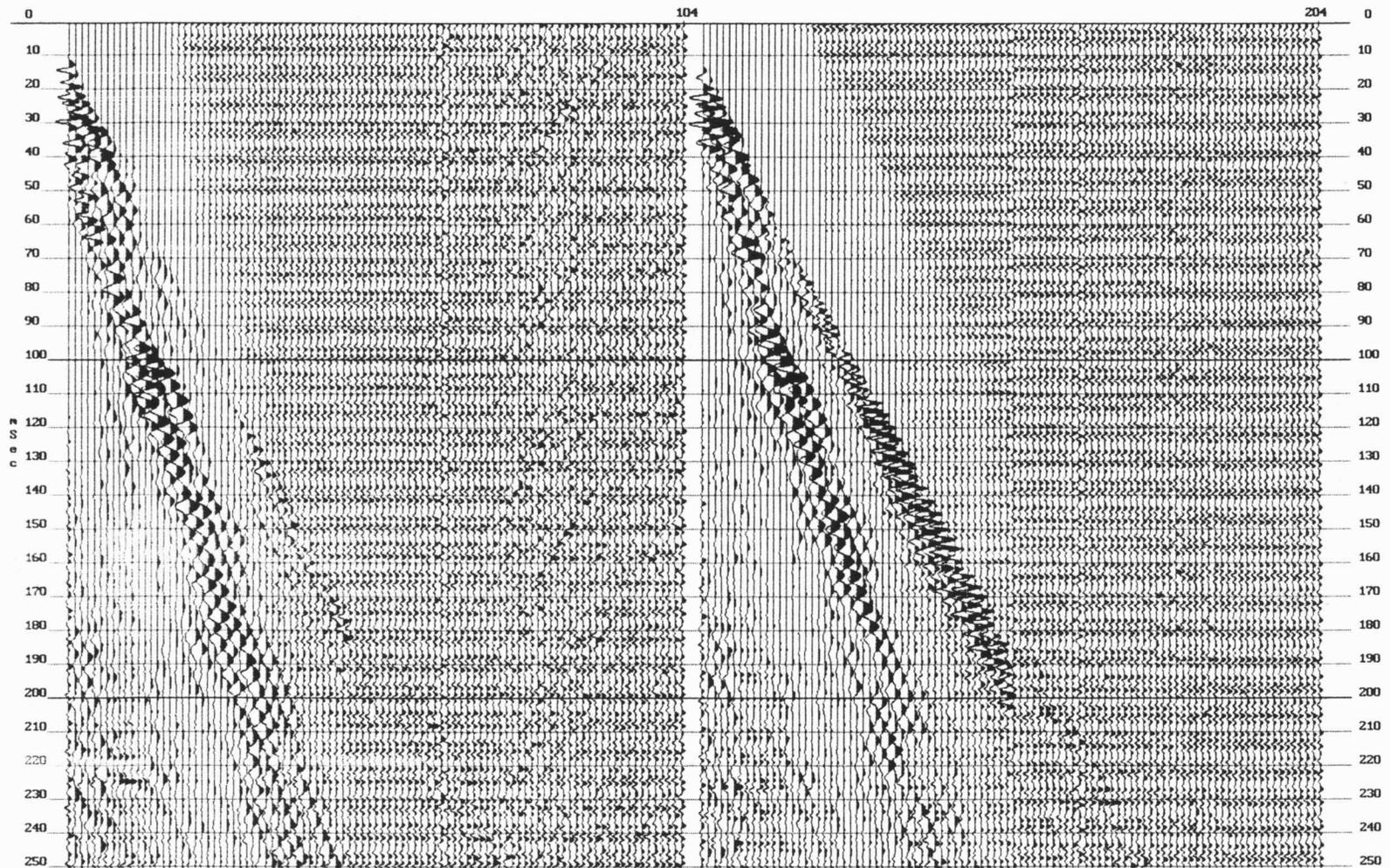
Figure 6
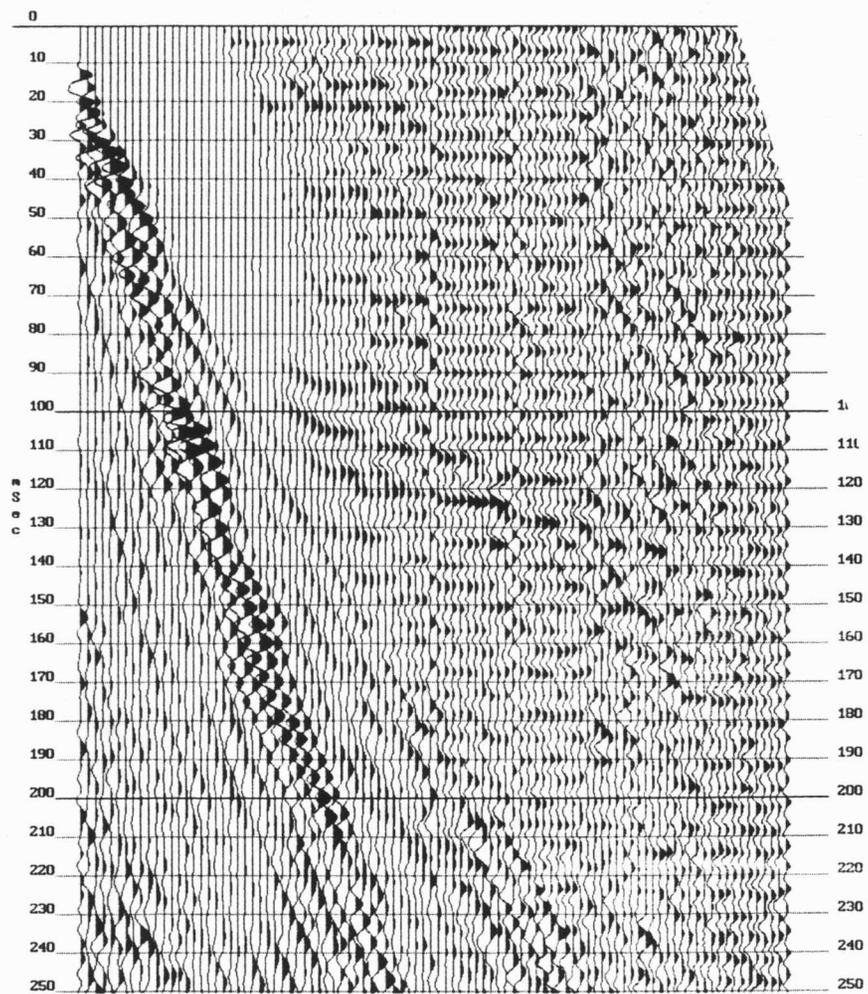
Figure 7
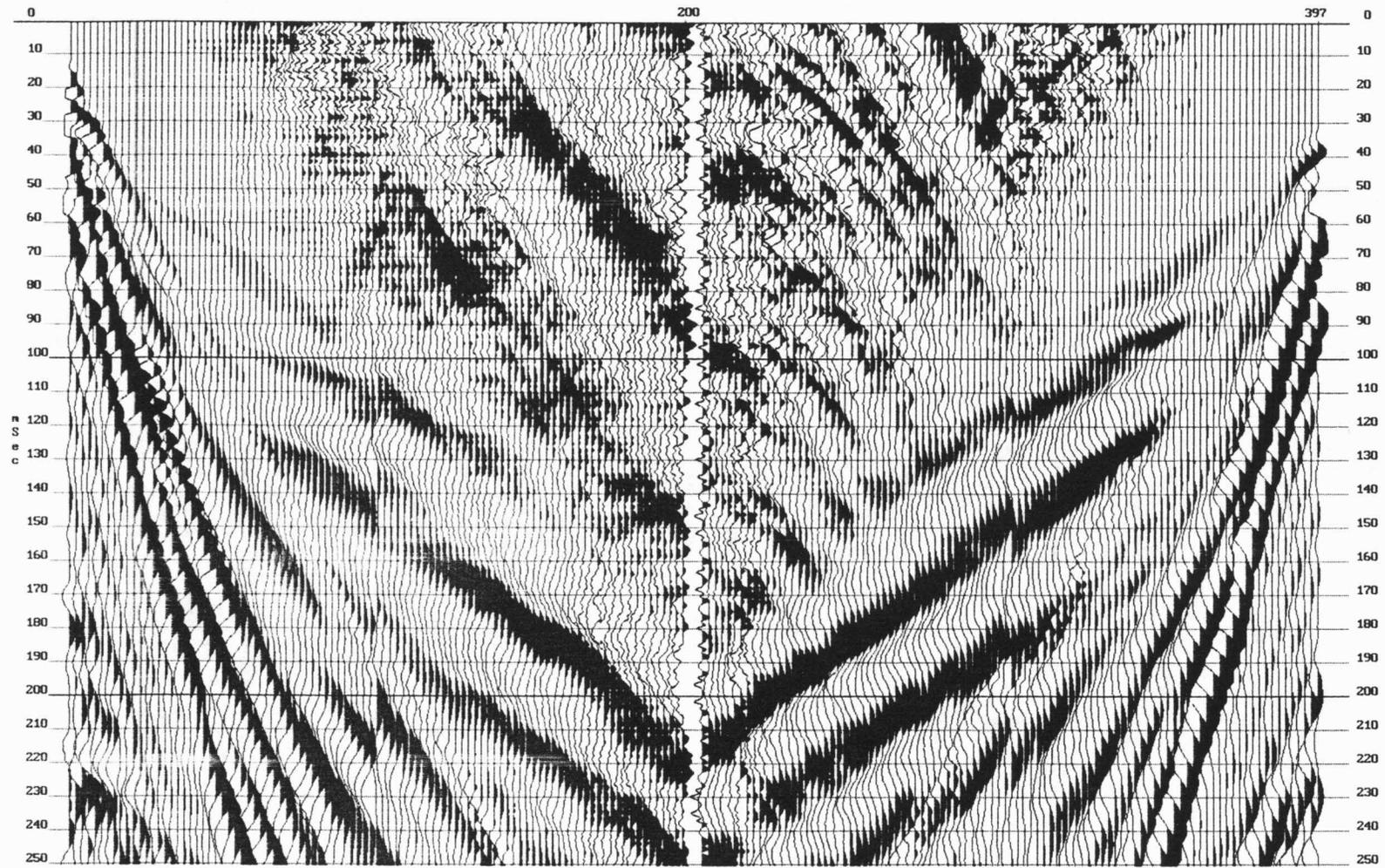
Figure 8
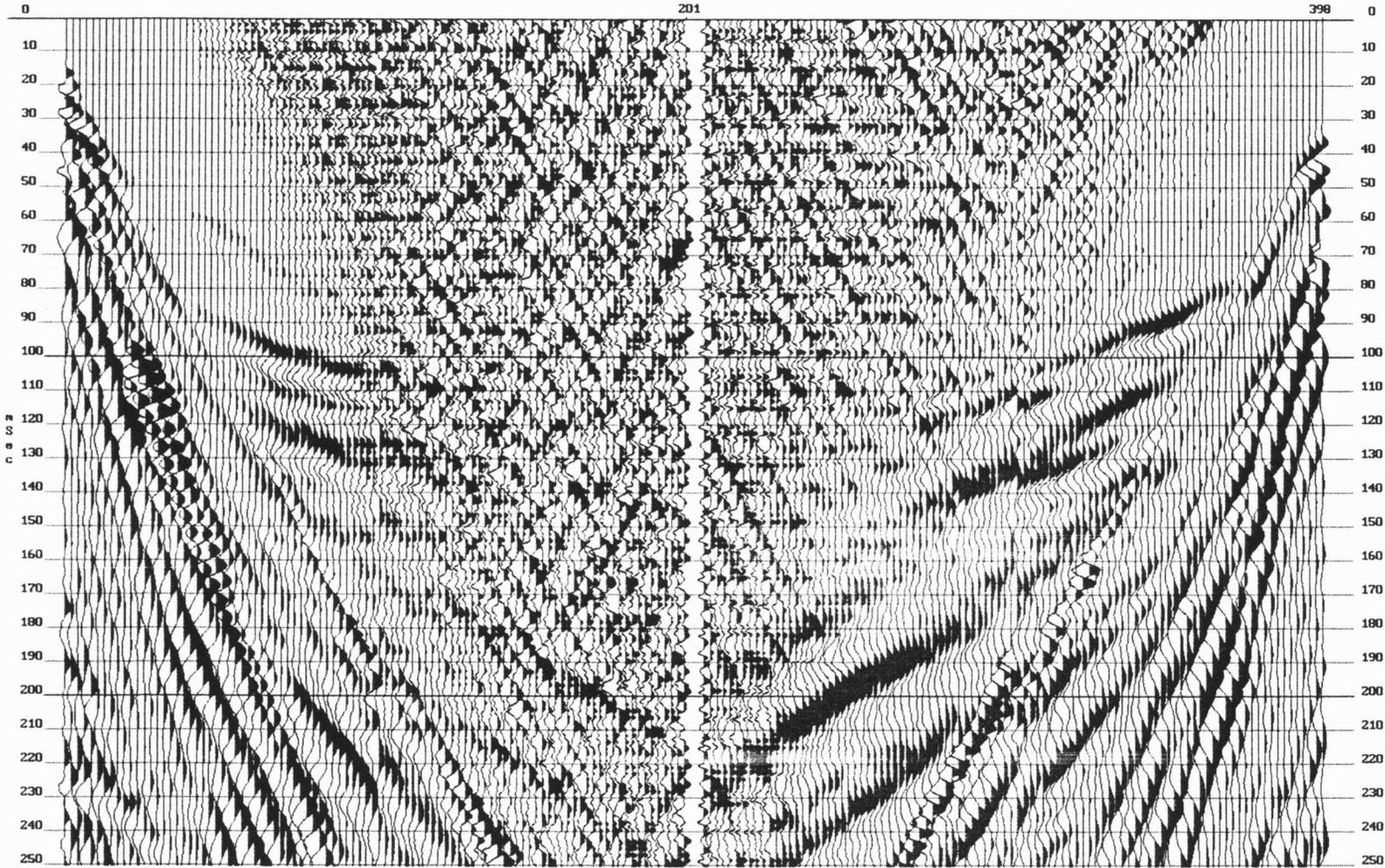
Figure 9
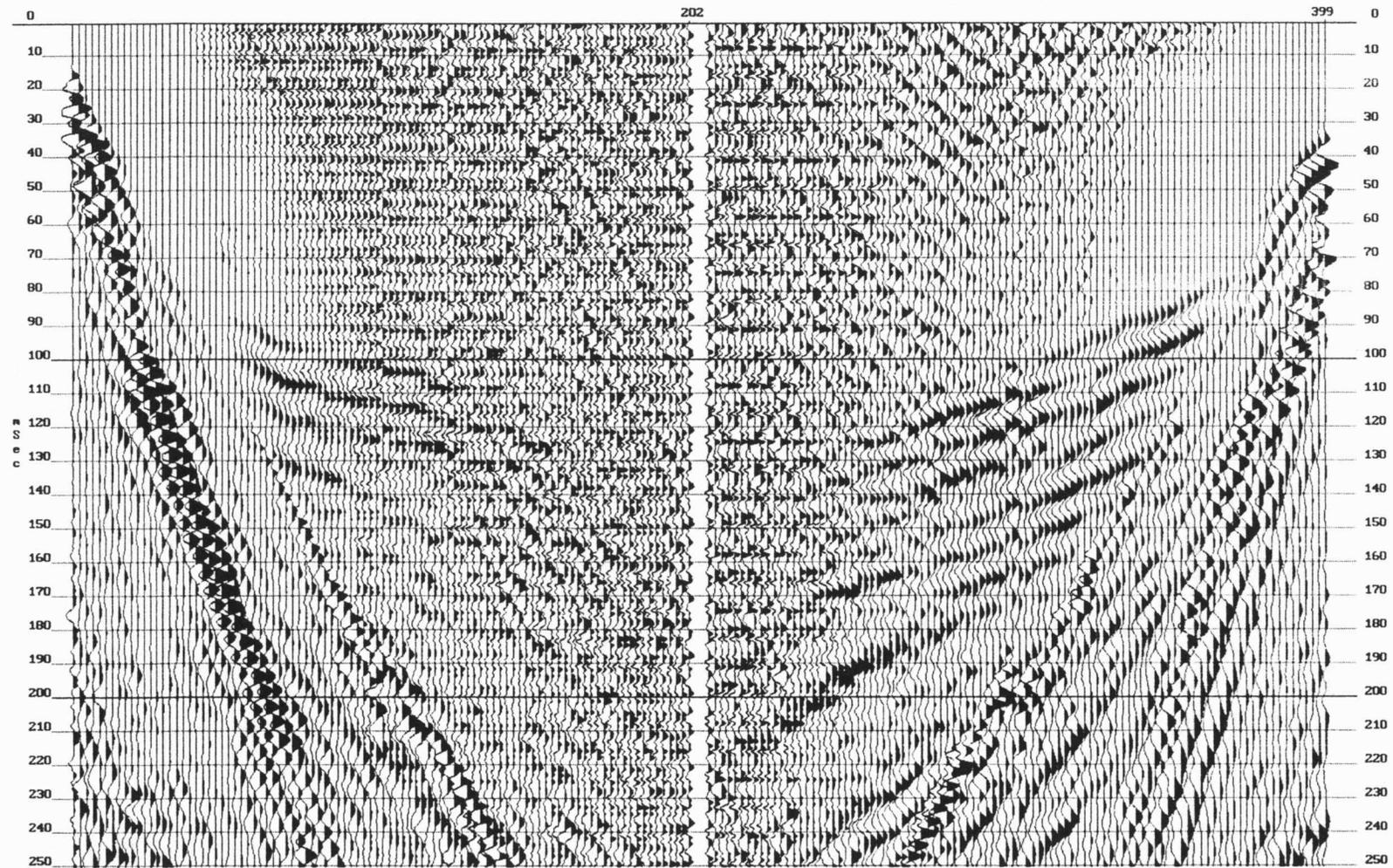
Figure 10
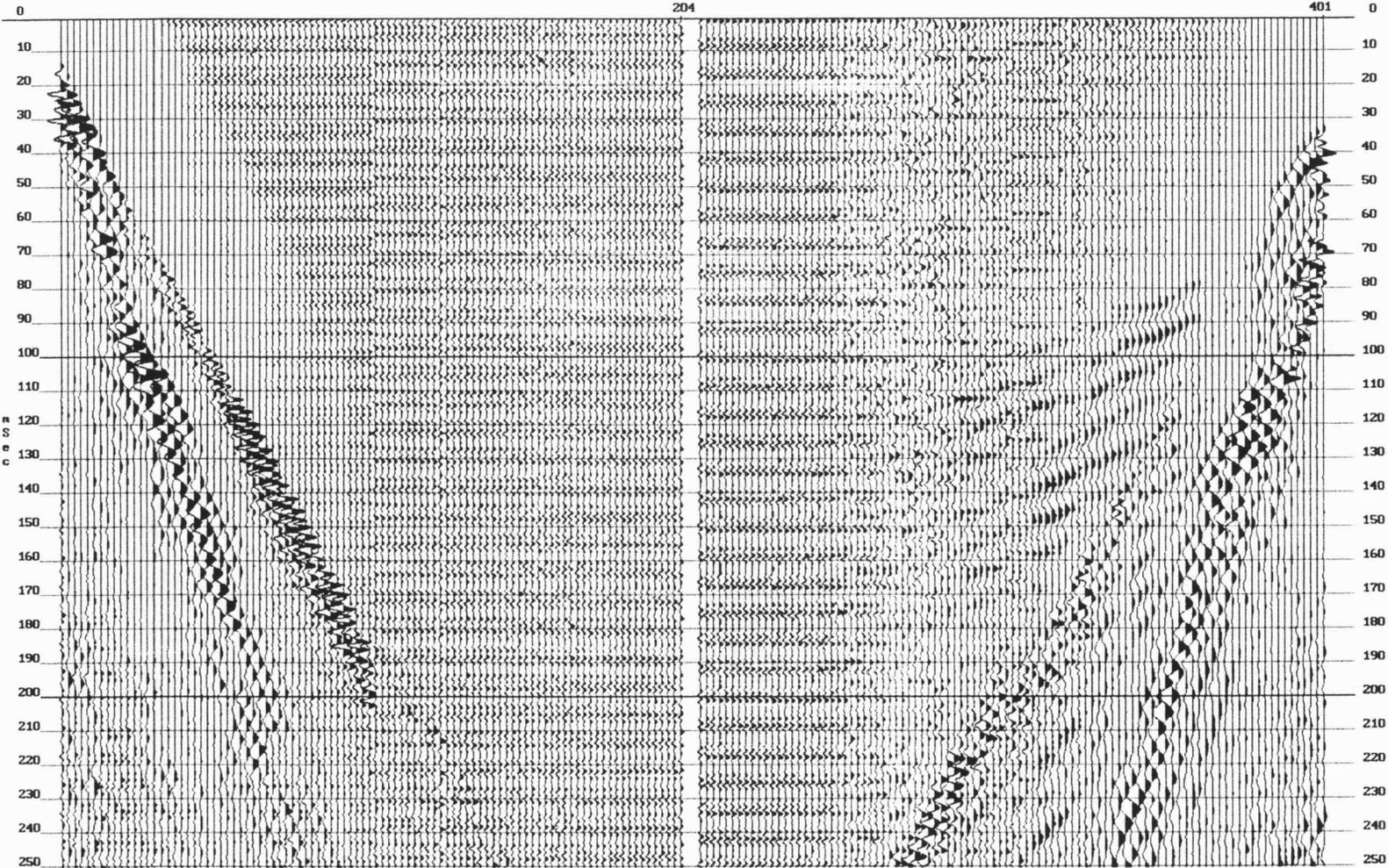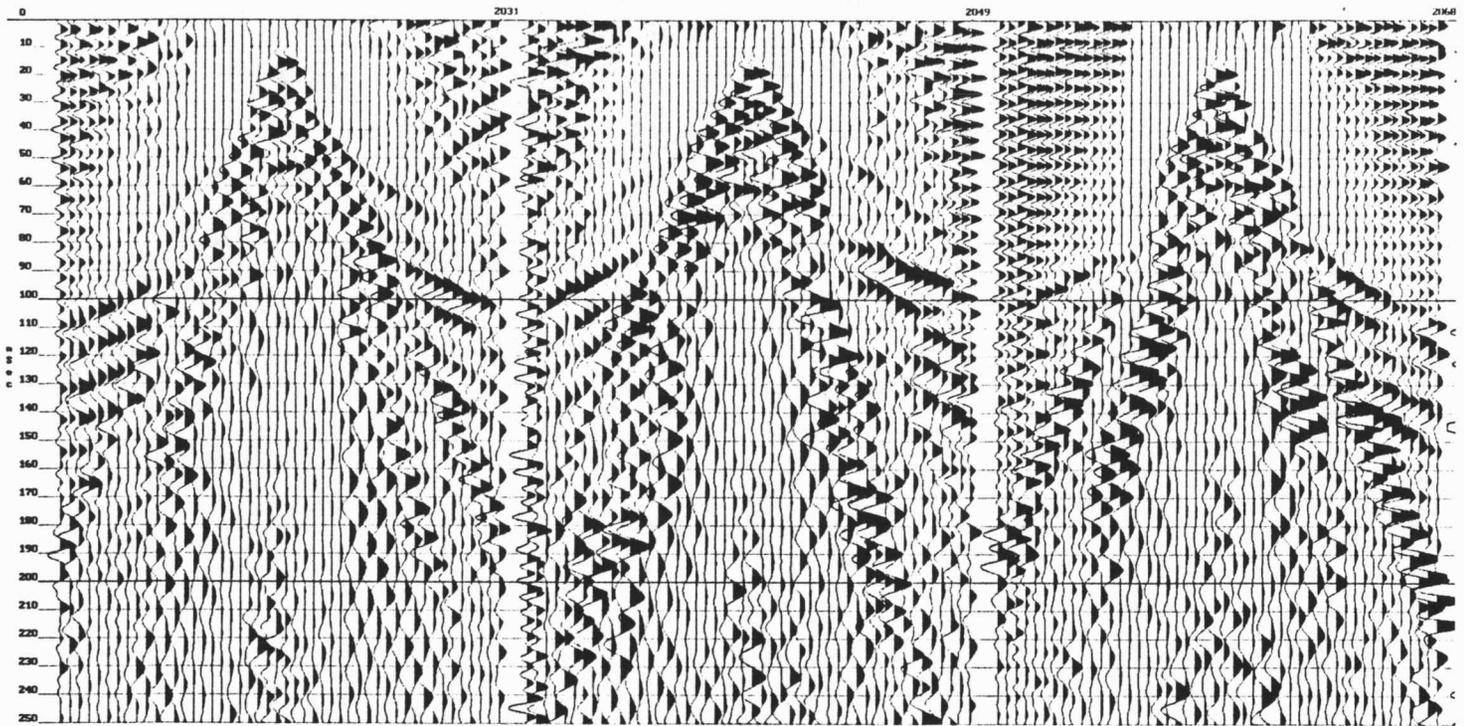
Figure 11
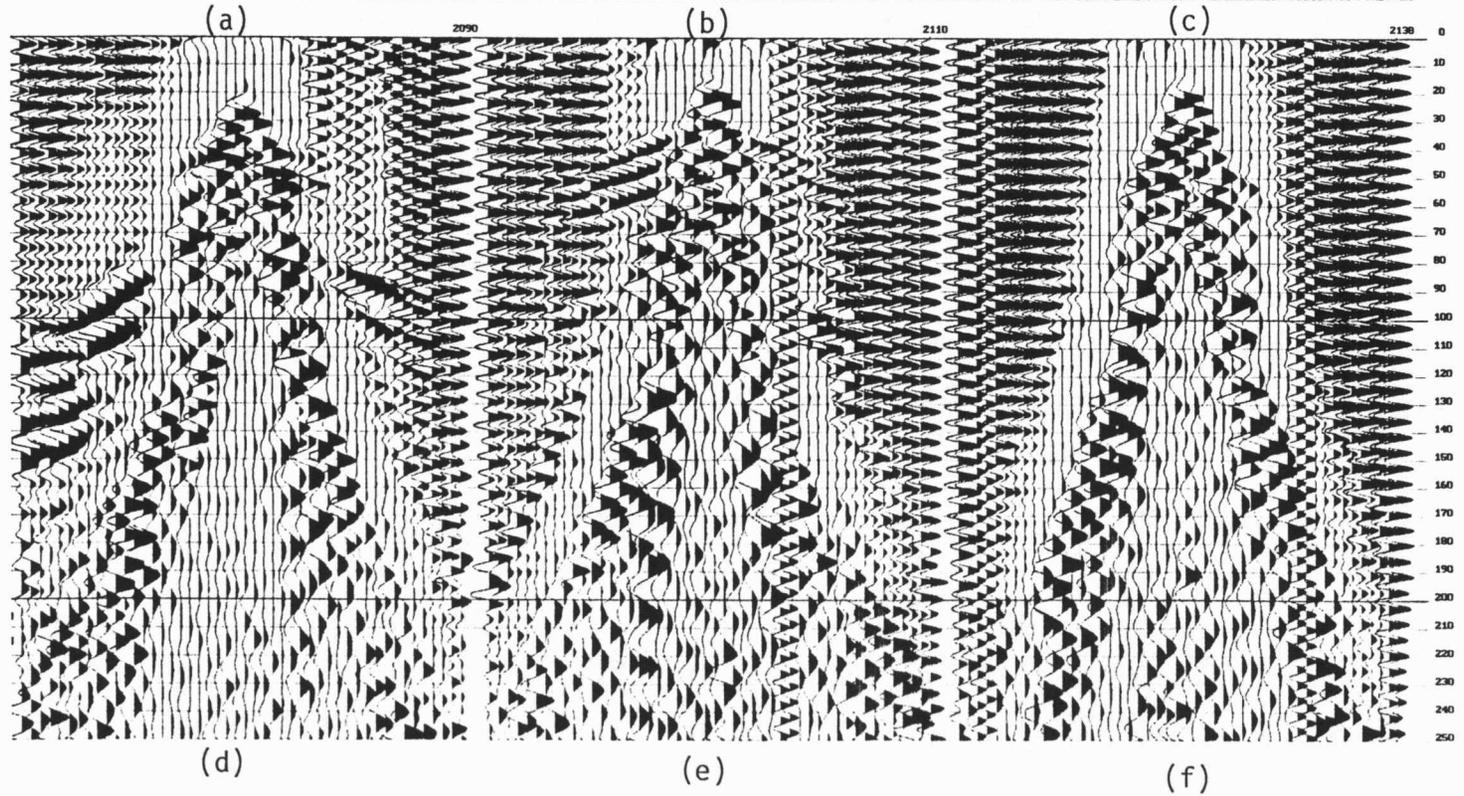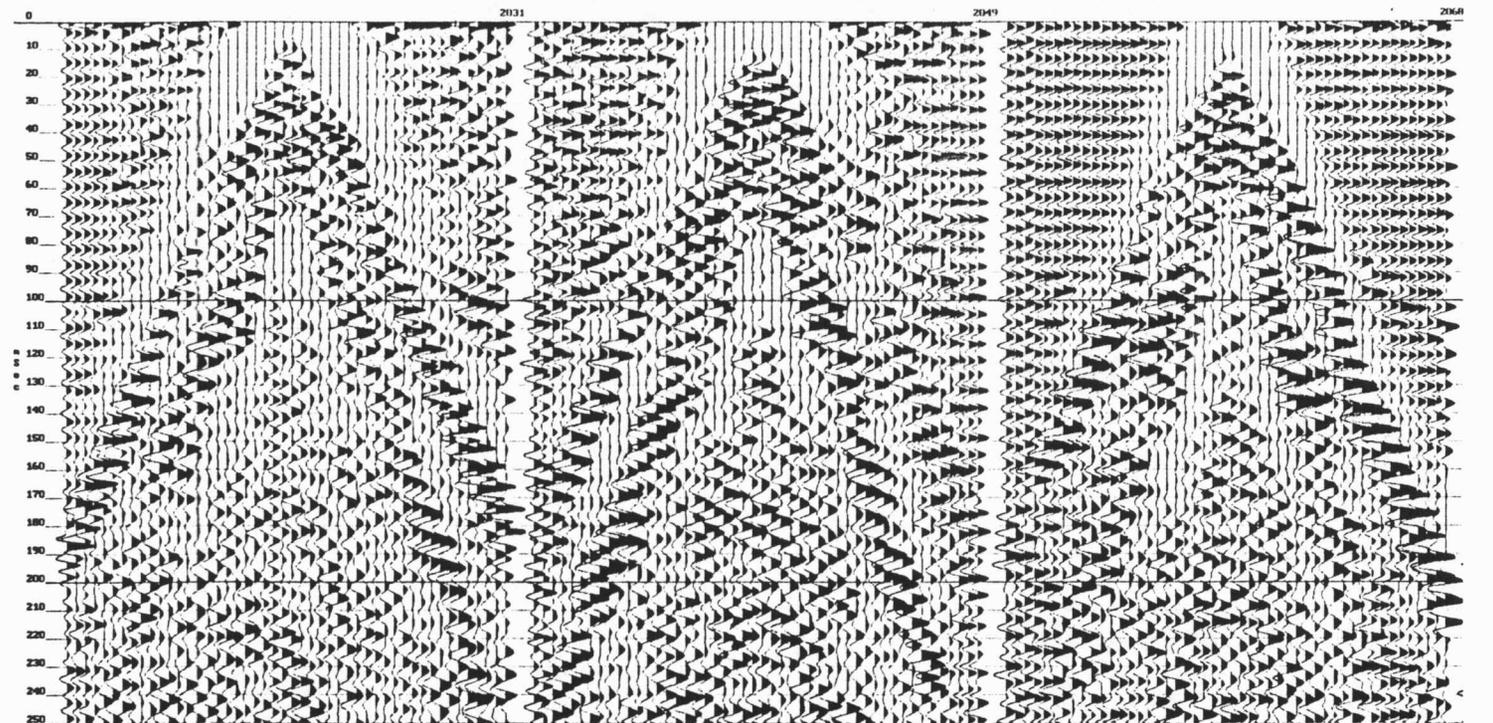
Figure 12

Figure 13

(a)   (b)   (c)

(d)   (e)   (f)

Figure 14

(a)   (b)   (c)

(d)   (e)   (f)
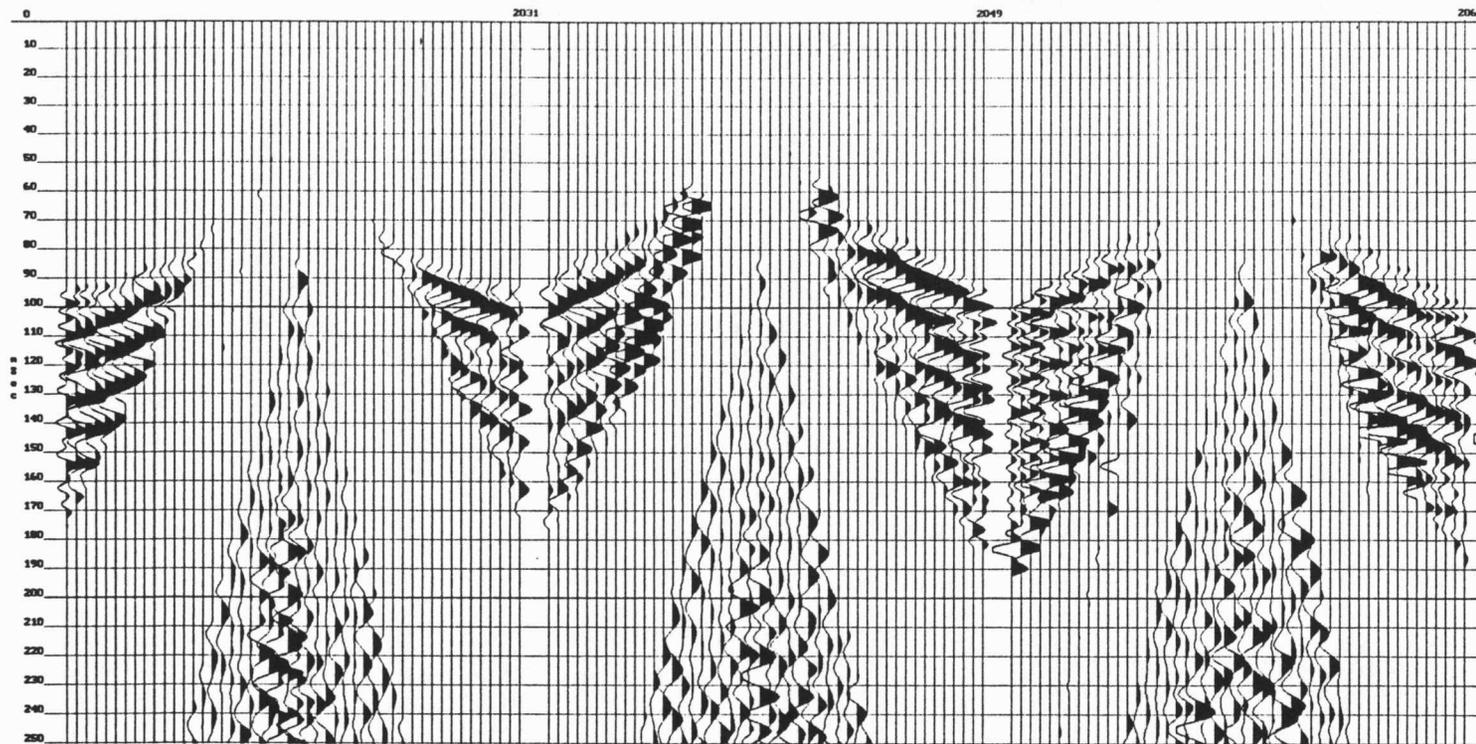
Figure 15
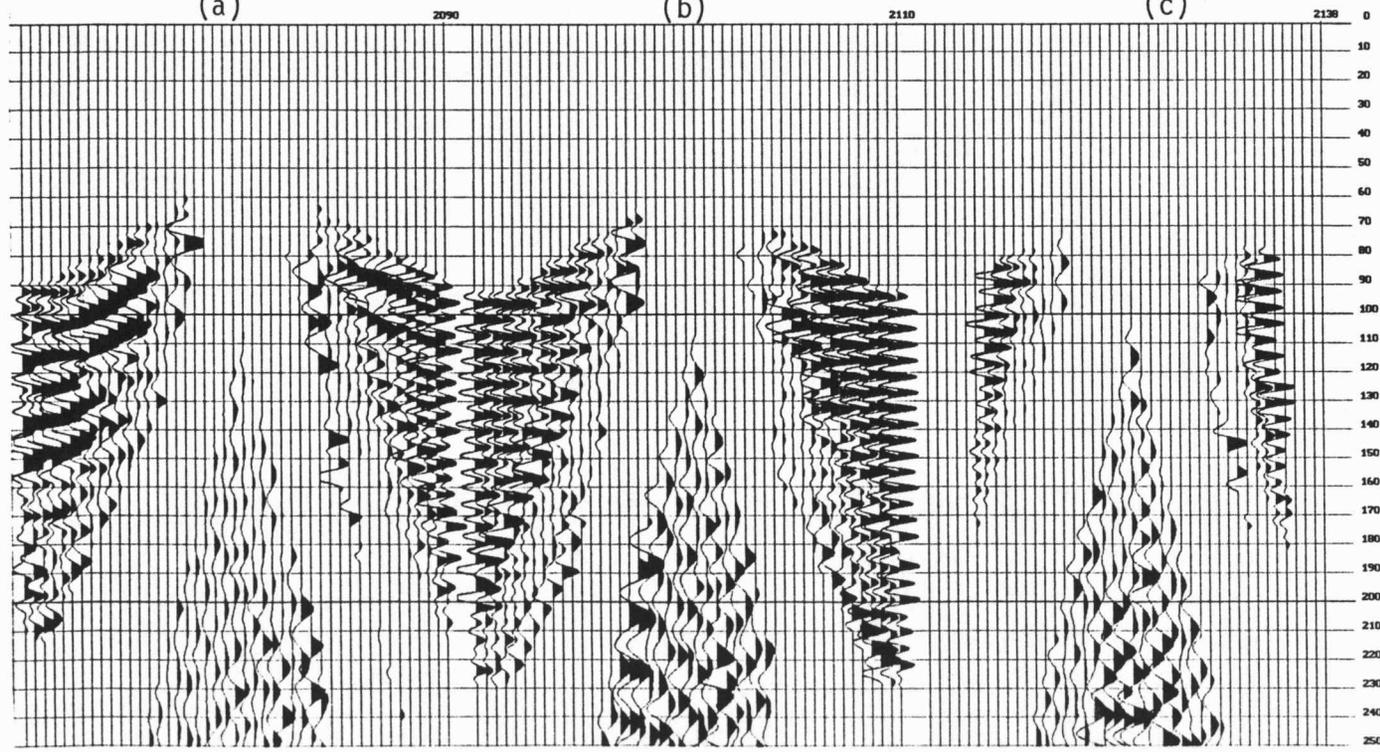
(a)   (b)   (c)

(d)   (e)   (f)
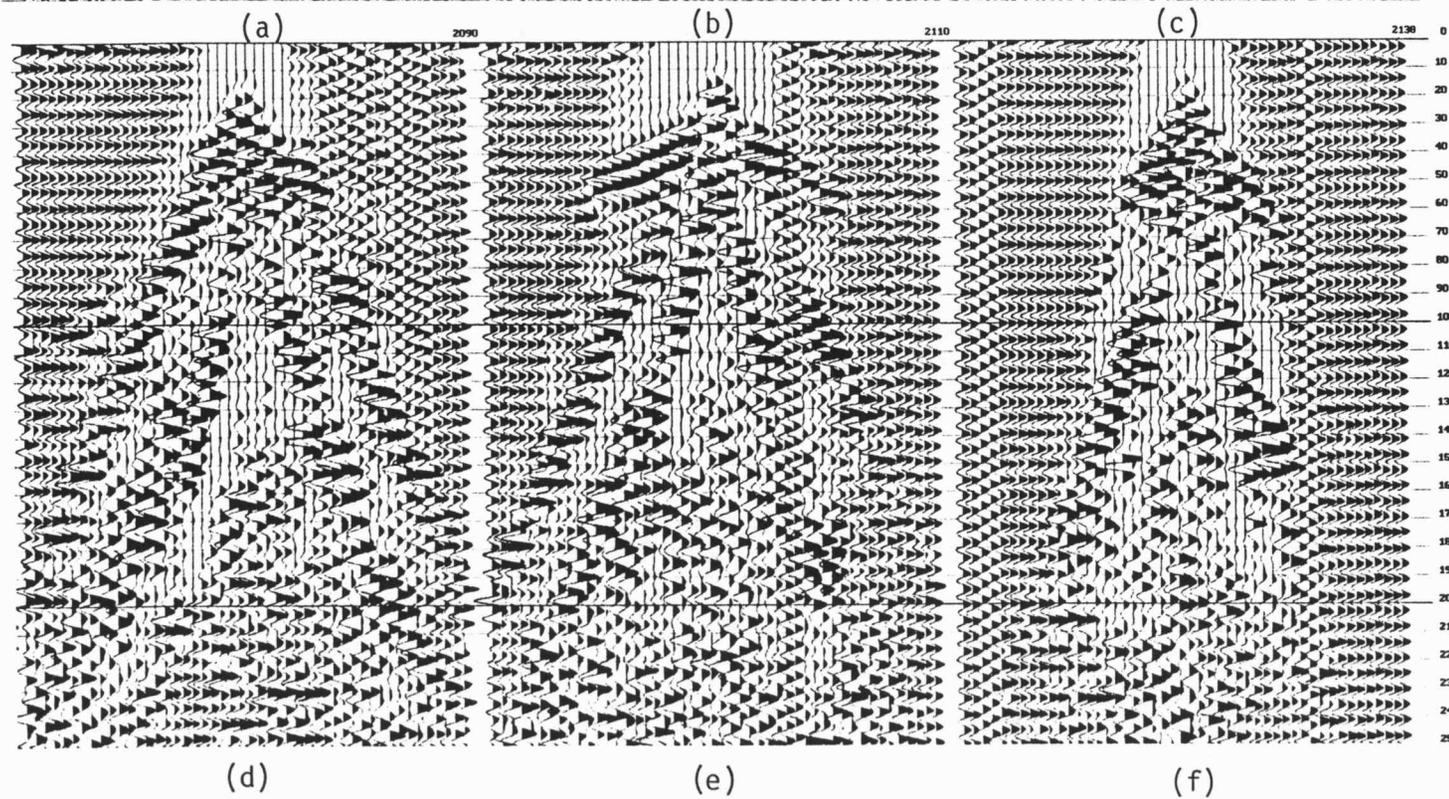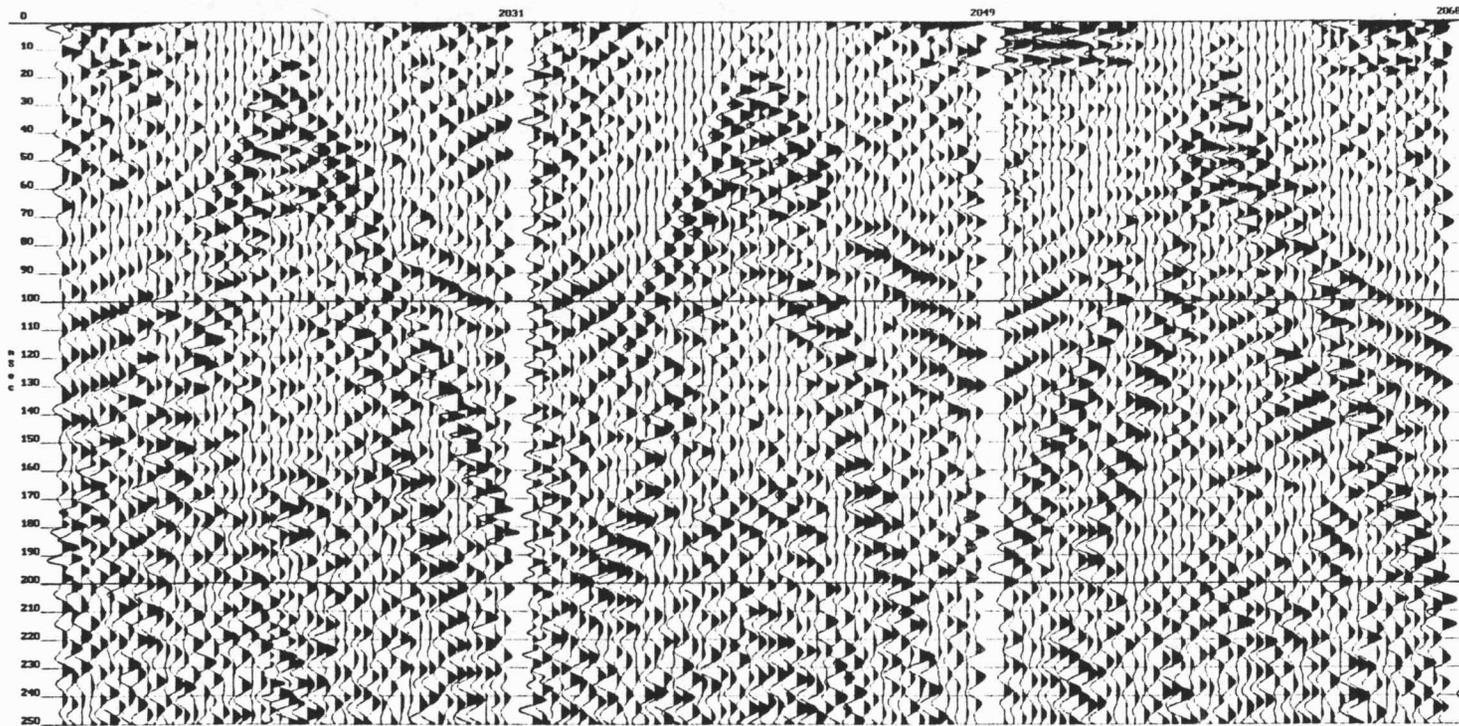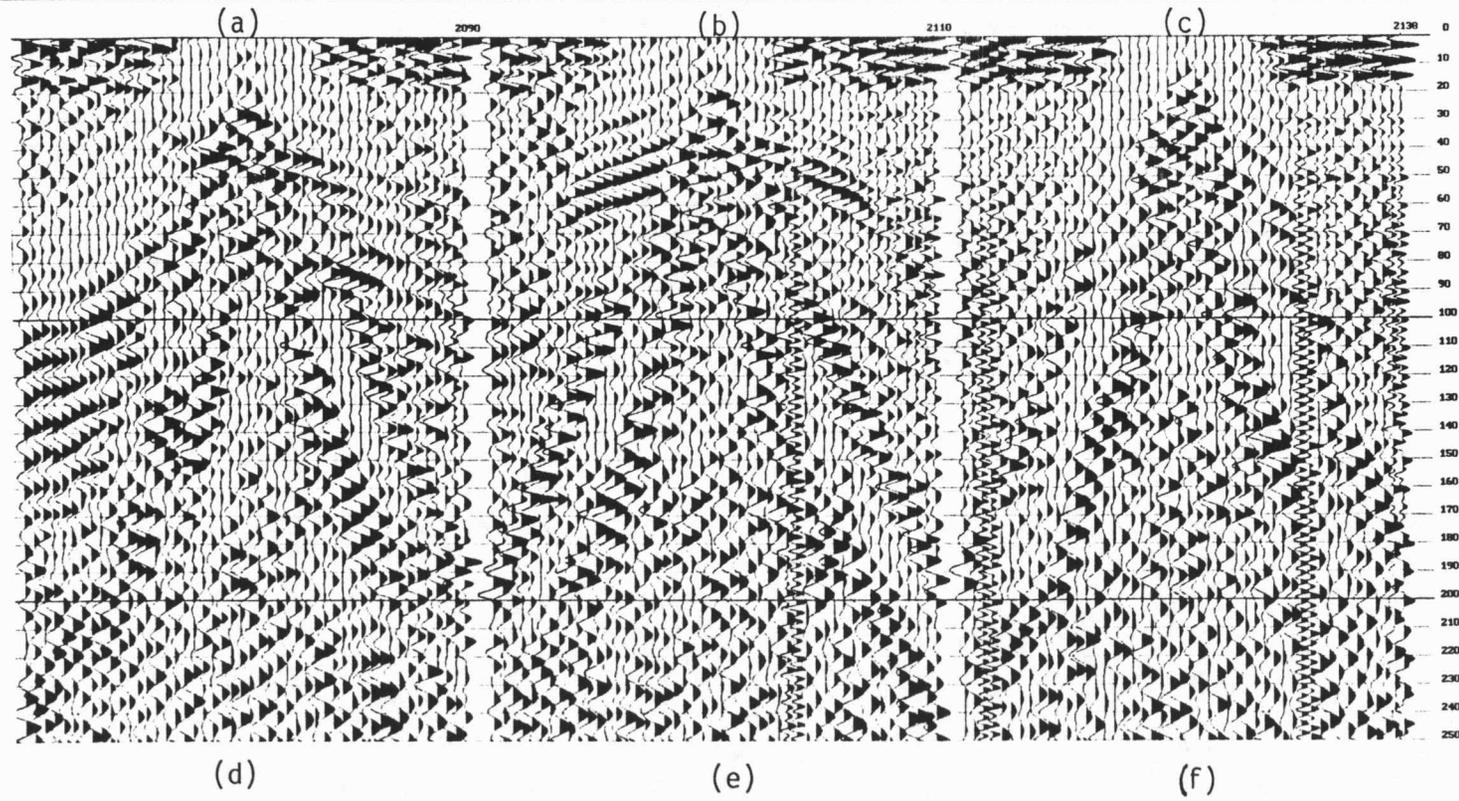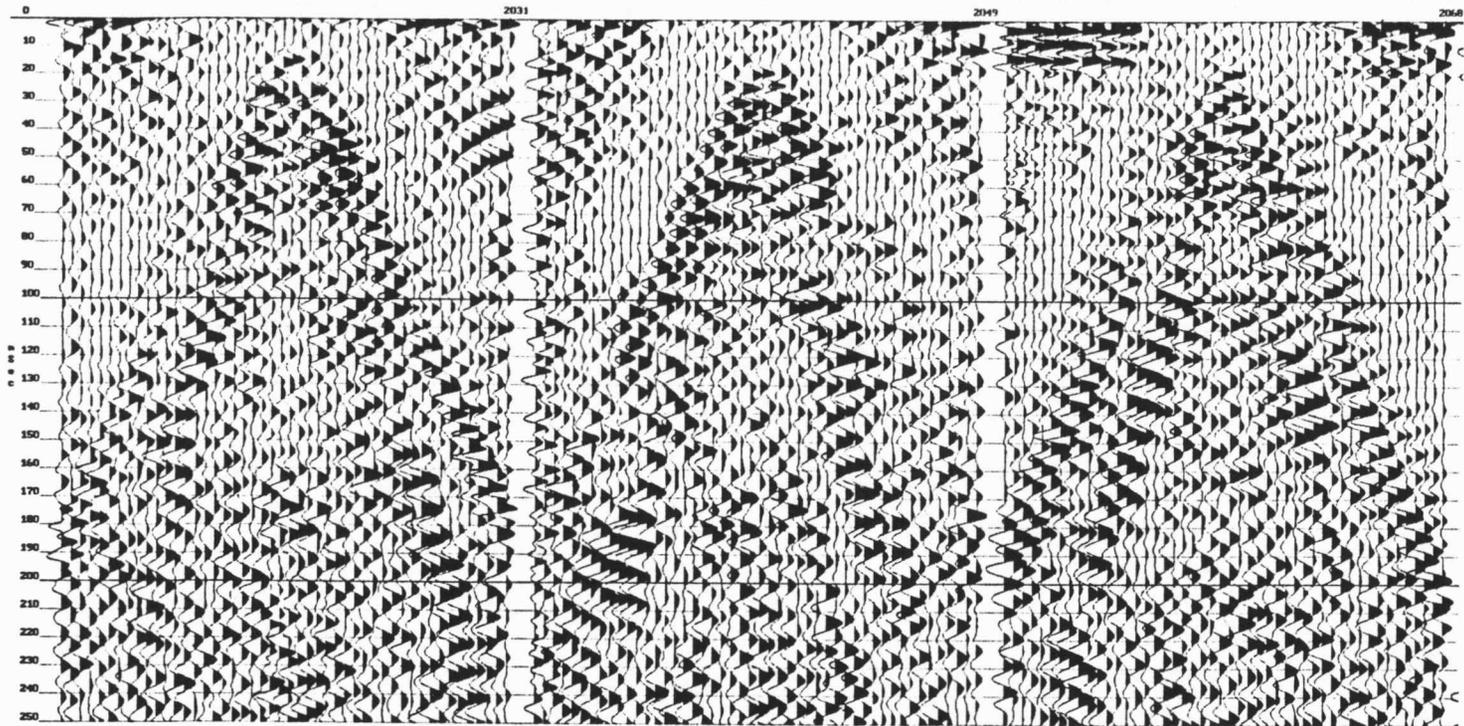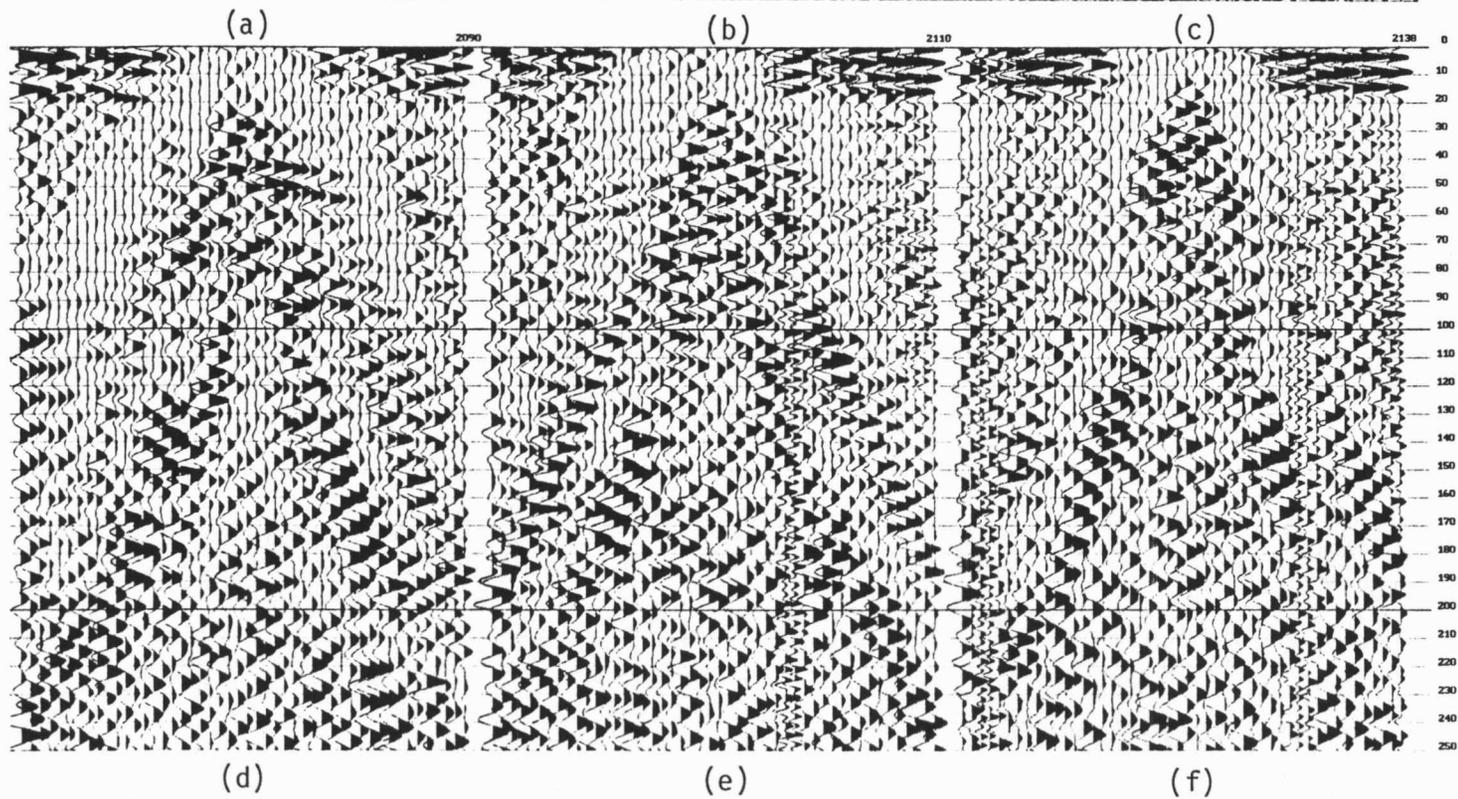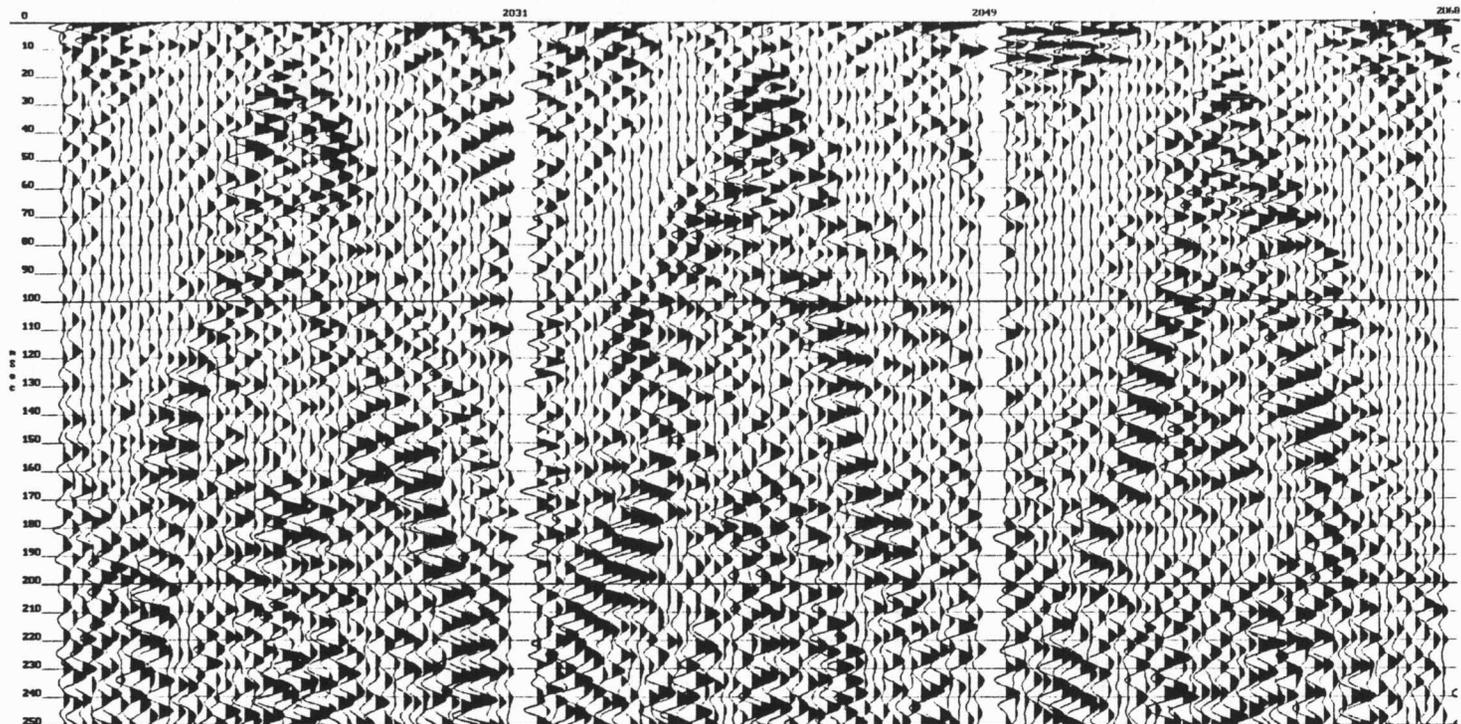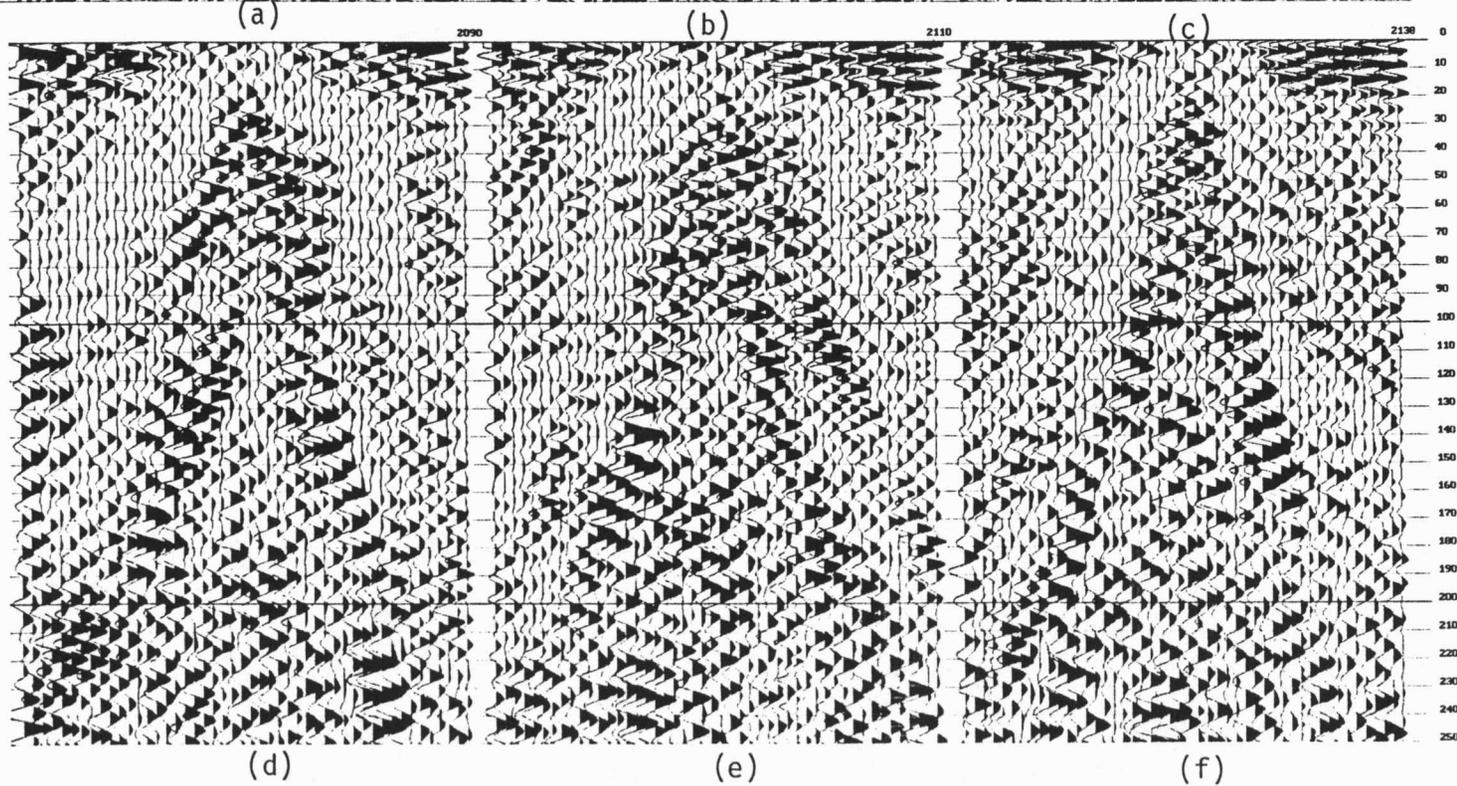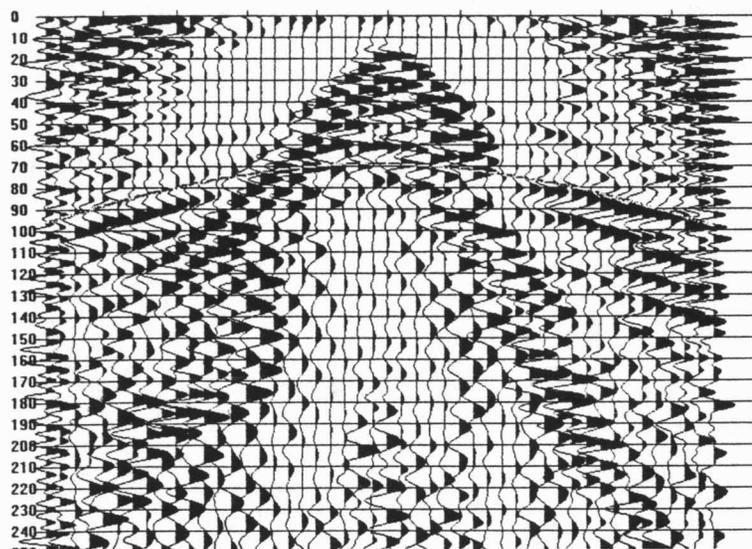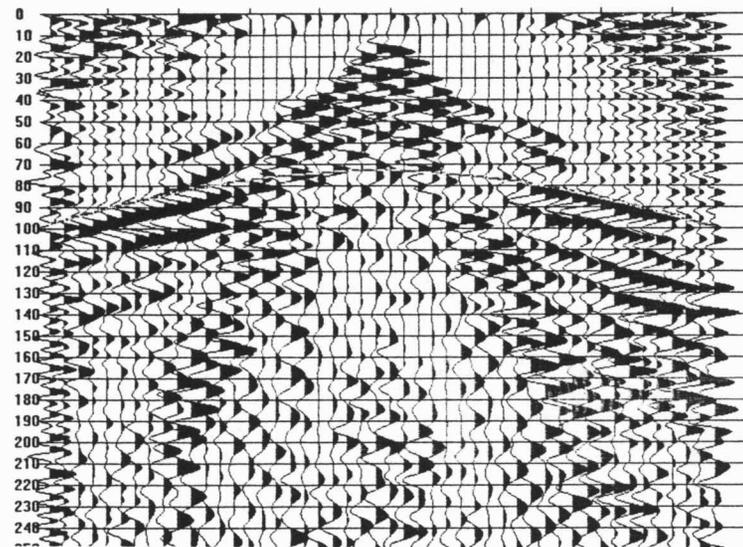
Figure 16

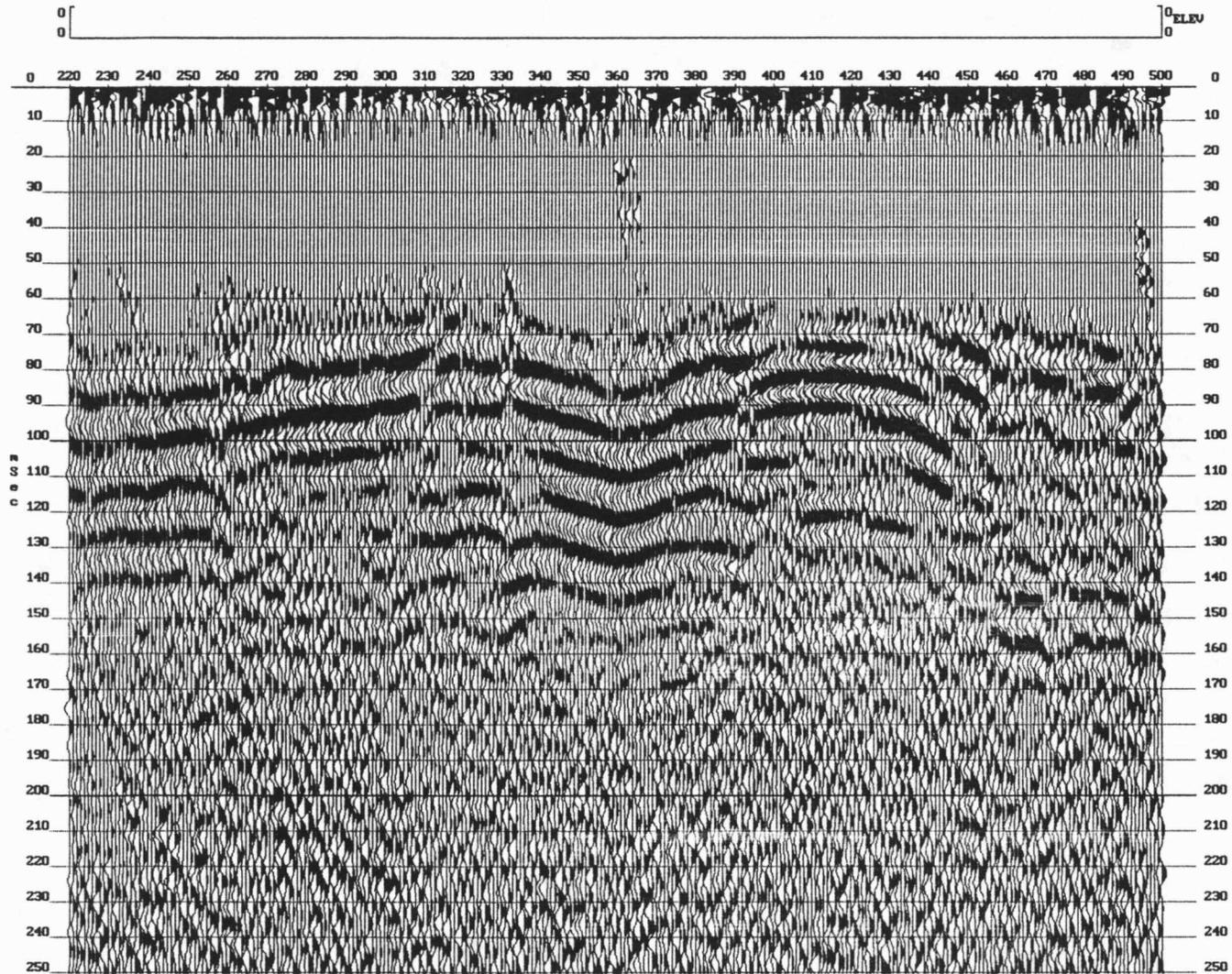
(a)   (b)
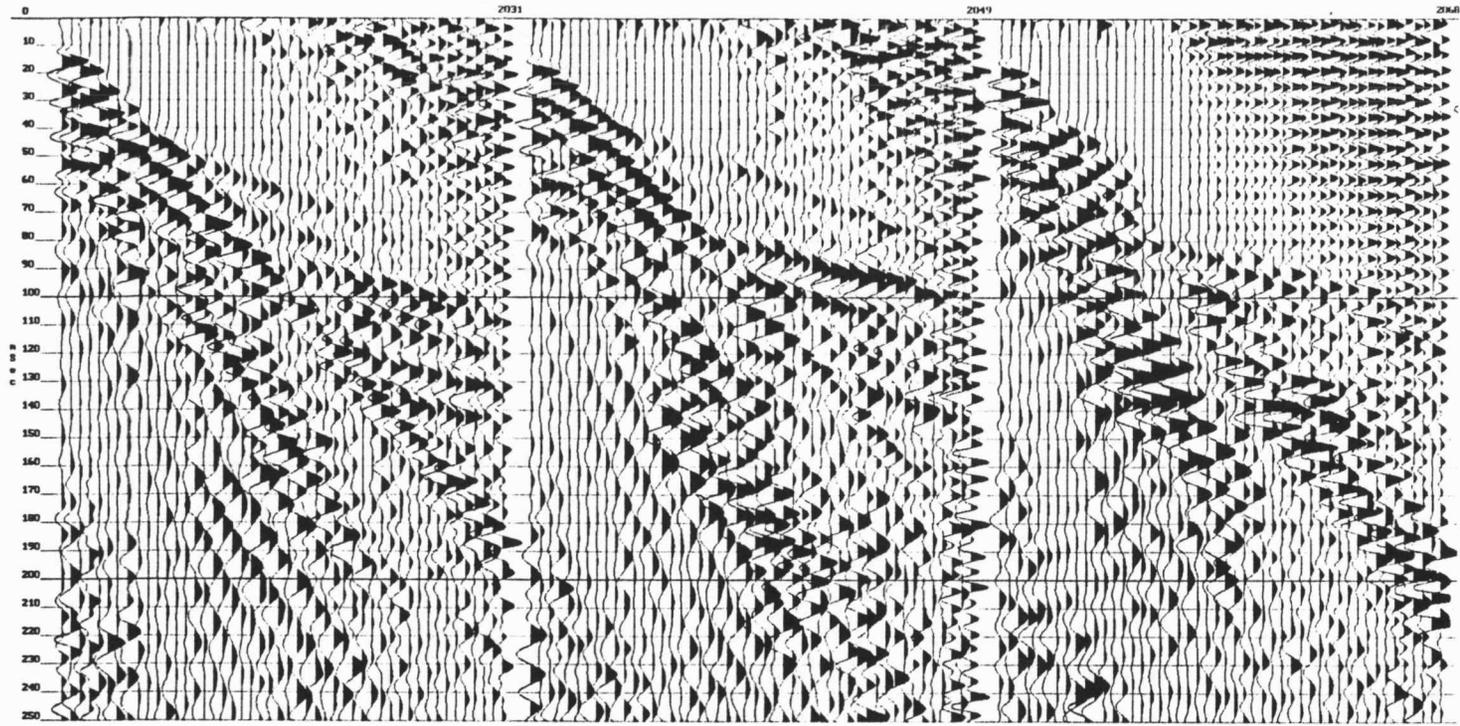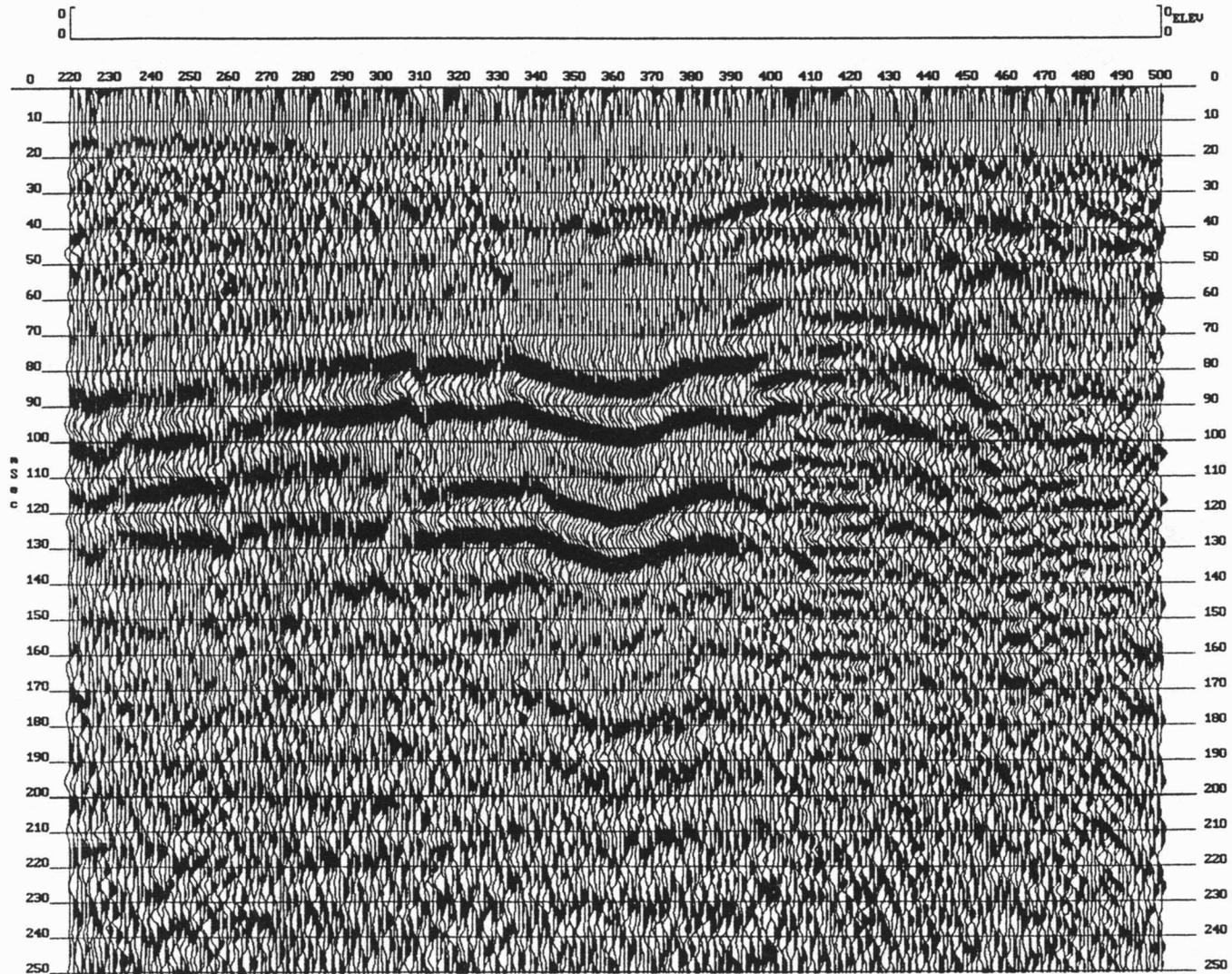
Figure 17
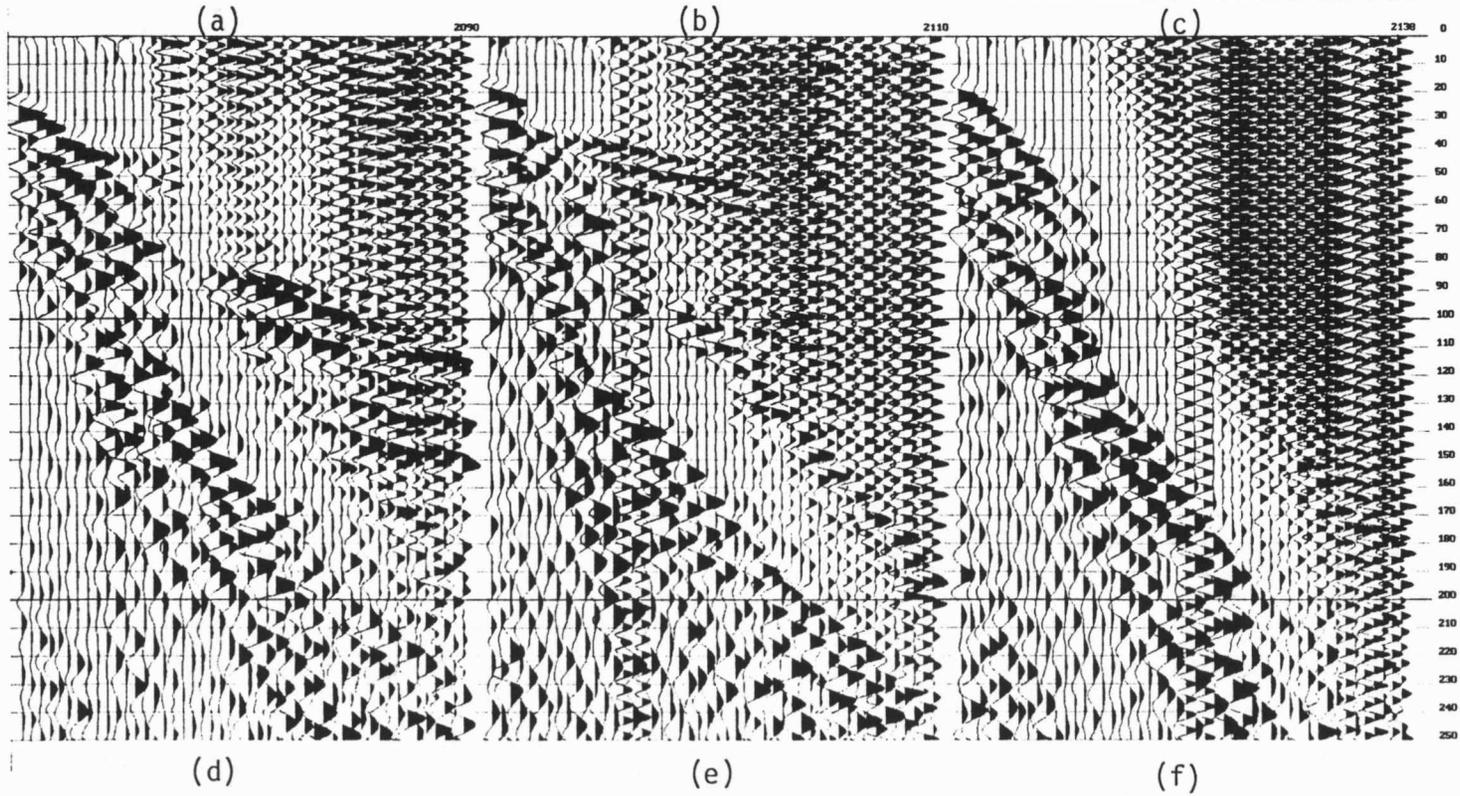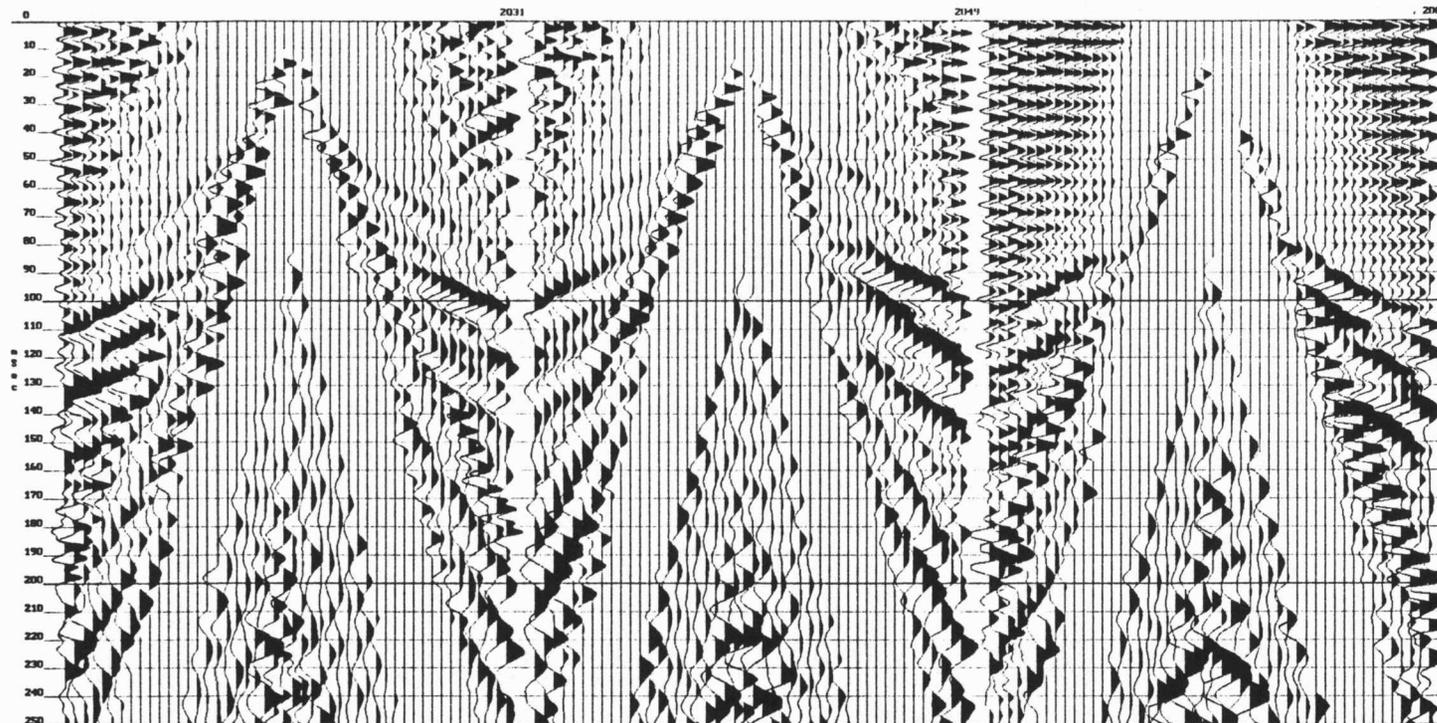
Figure 18
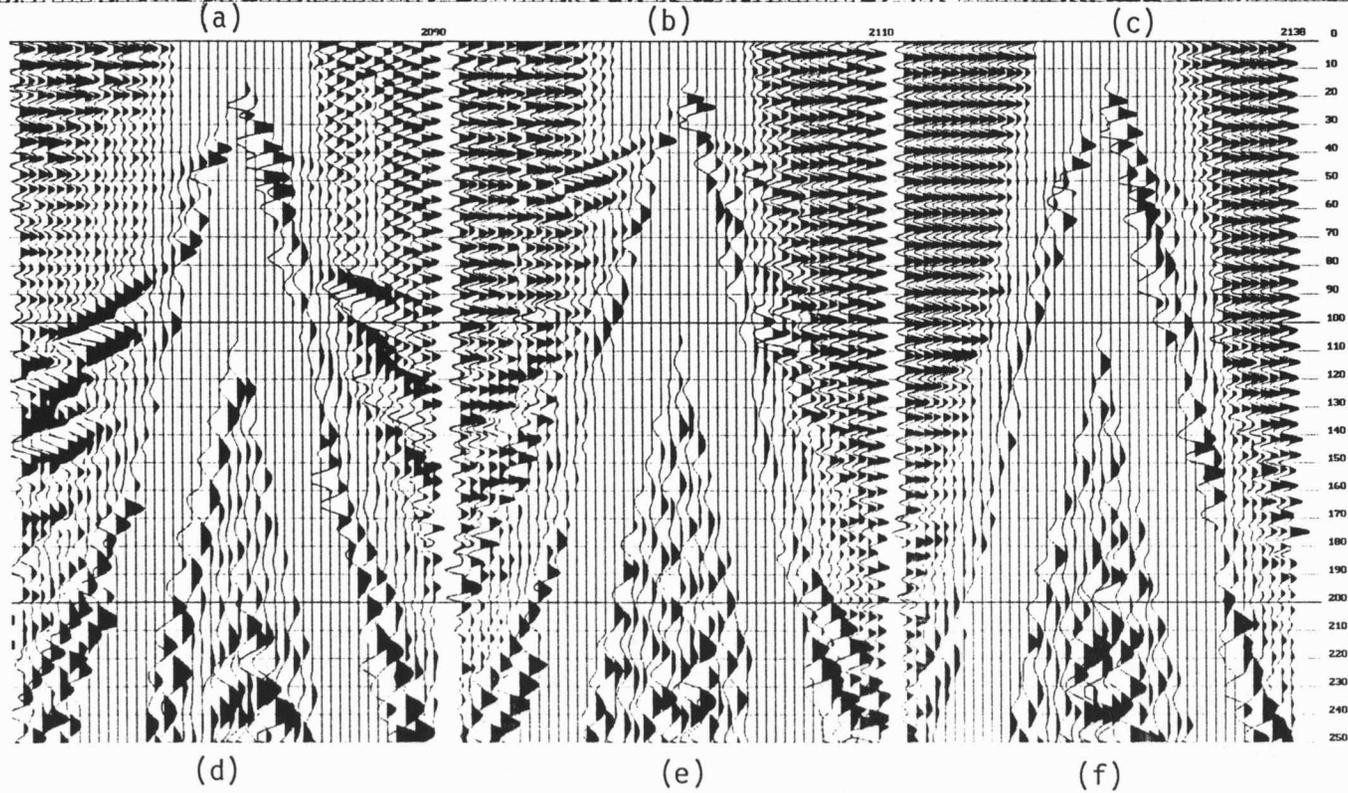
Figure 19

Figure 20

Figure 21
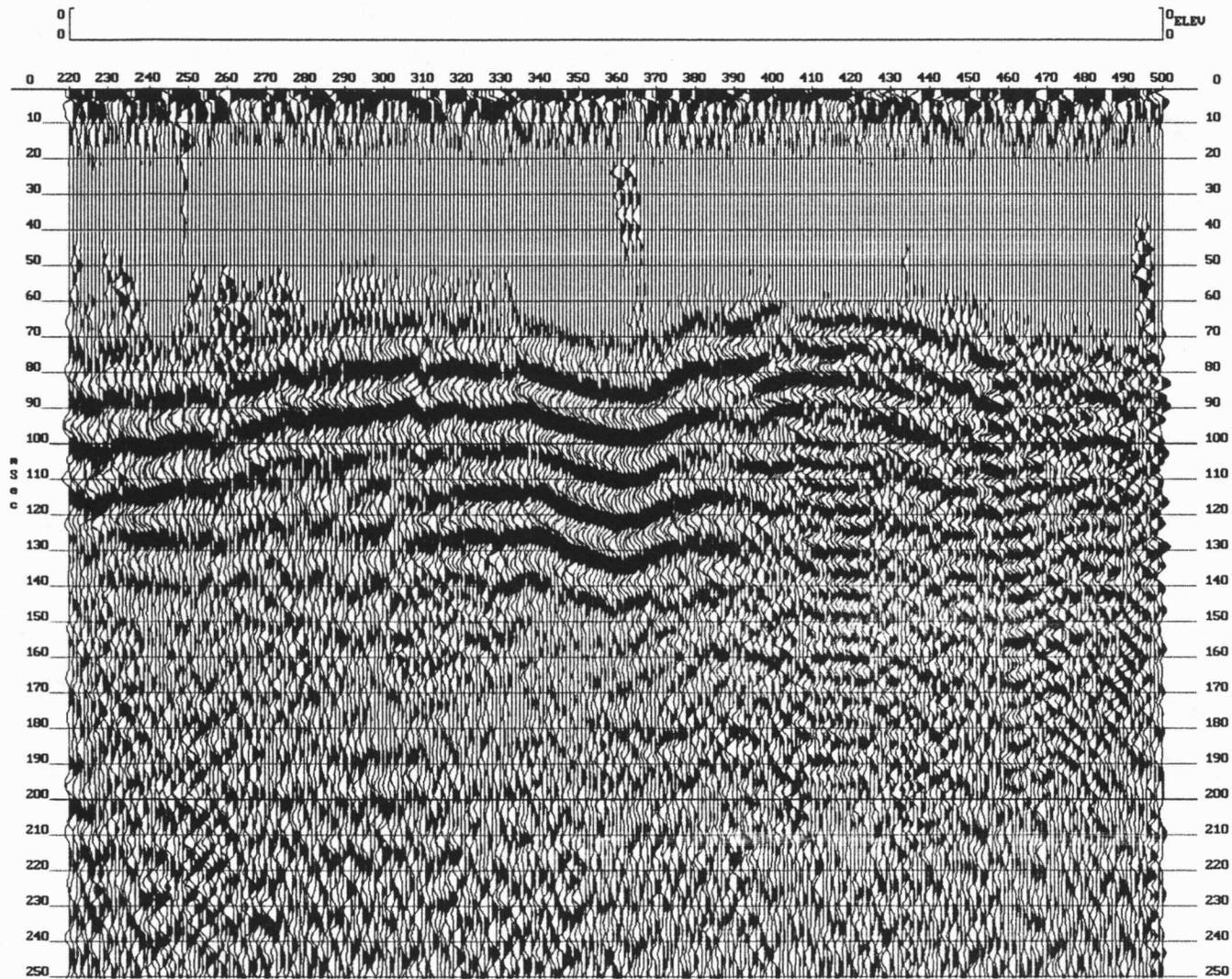
Figure 22
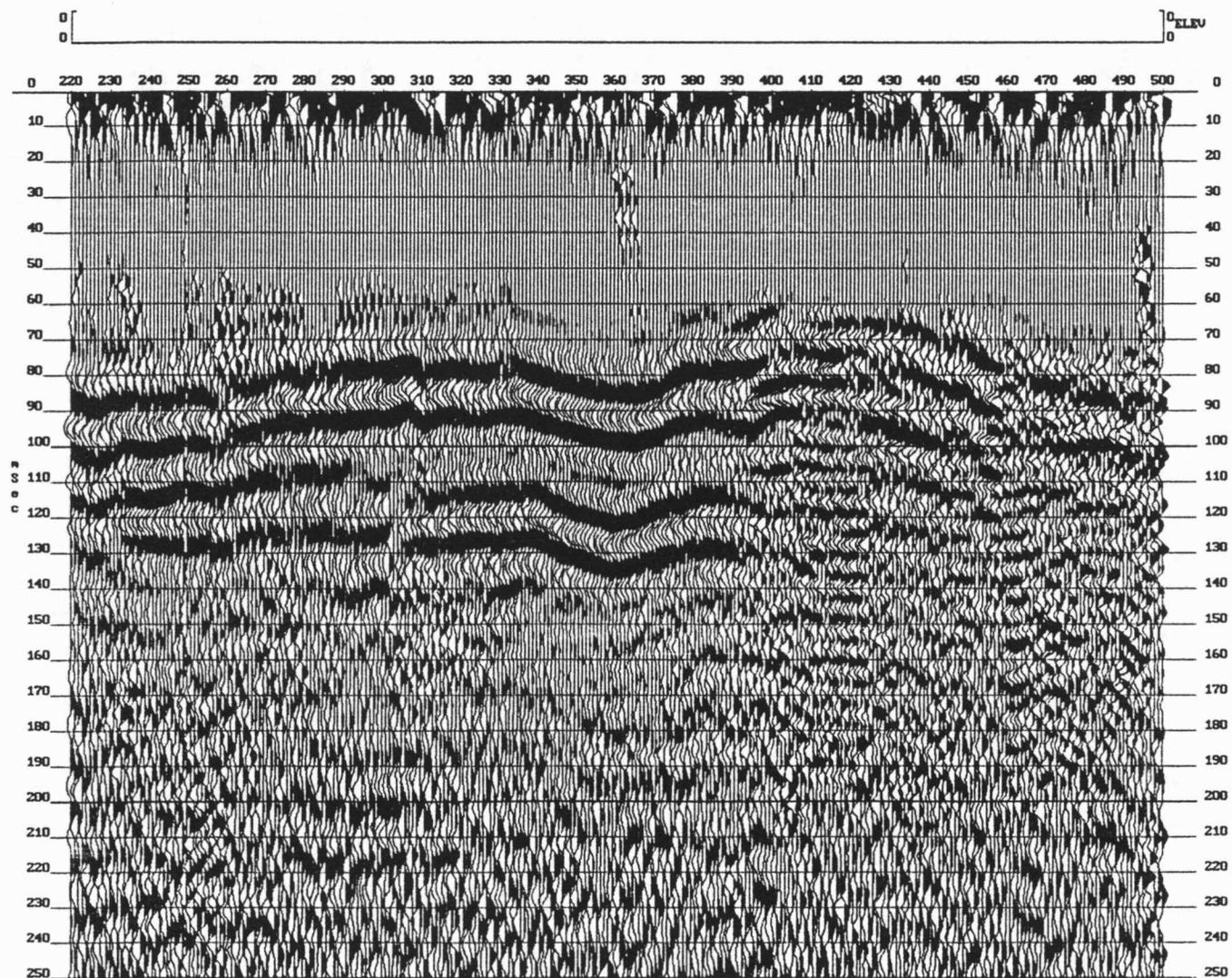
Figure 23

Figure 24
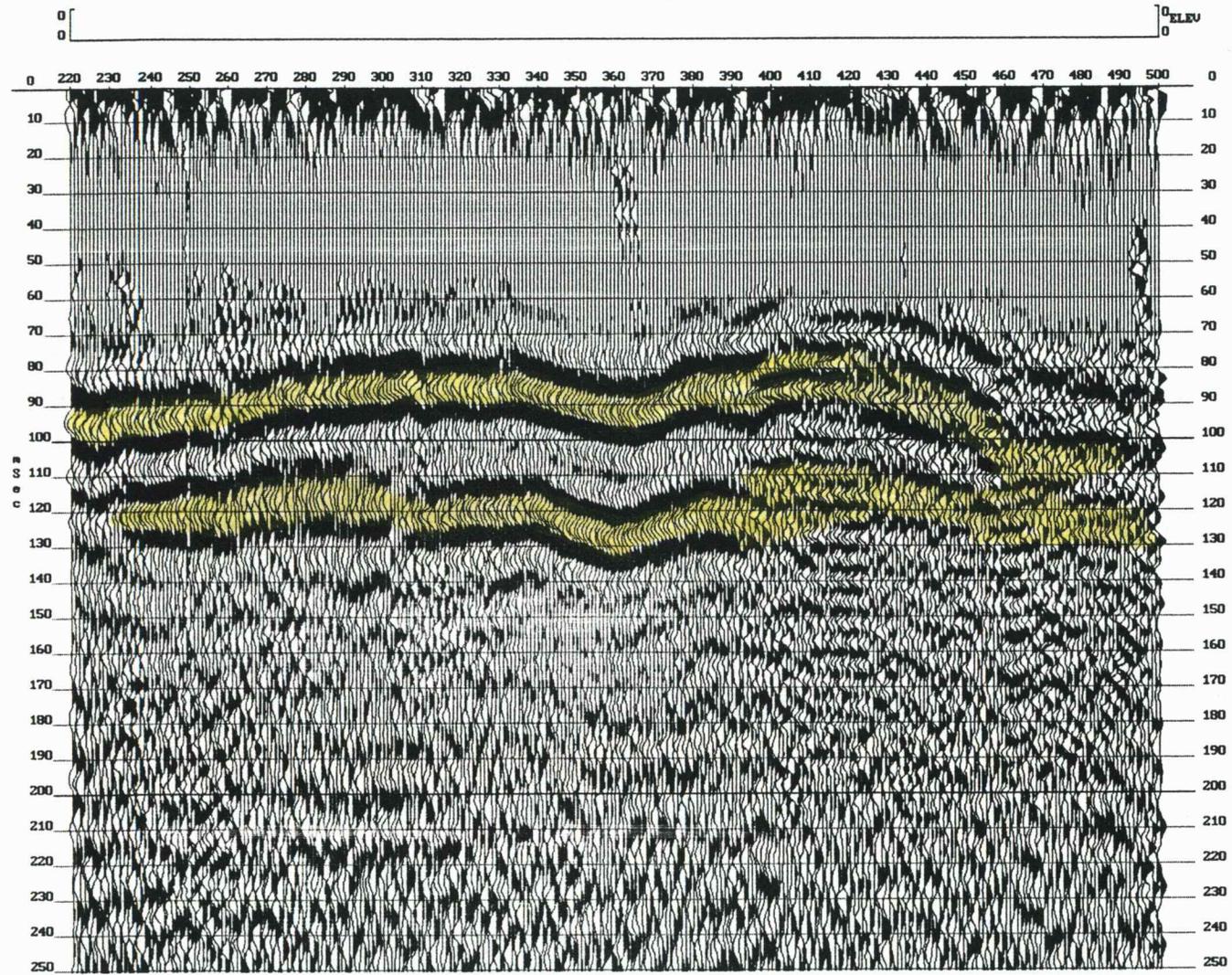
Figure 25

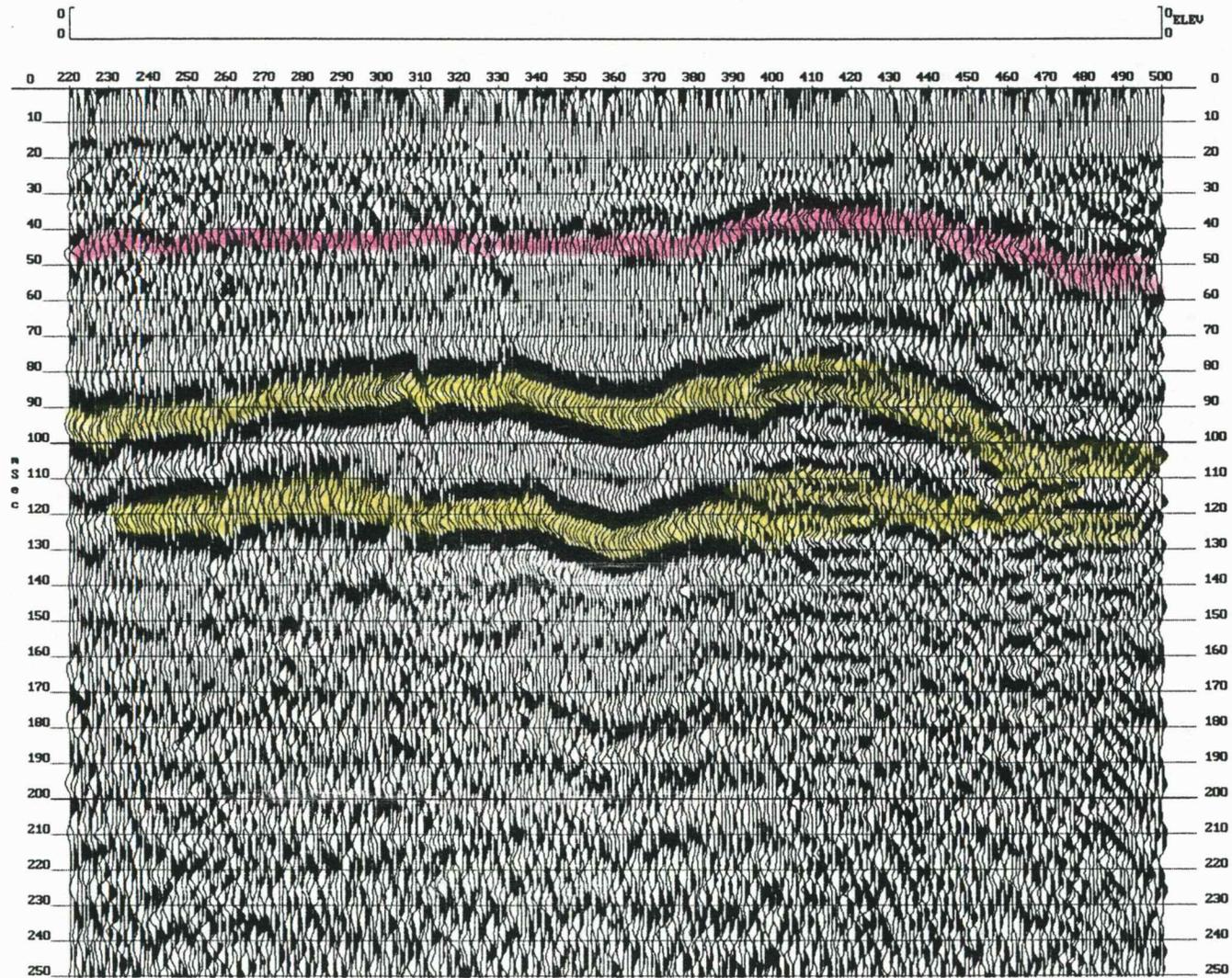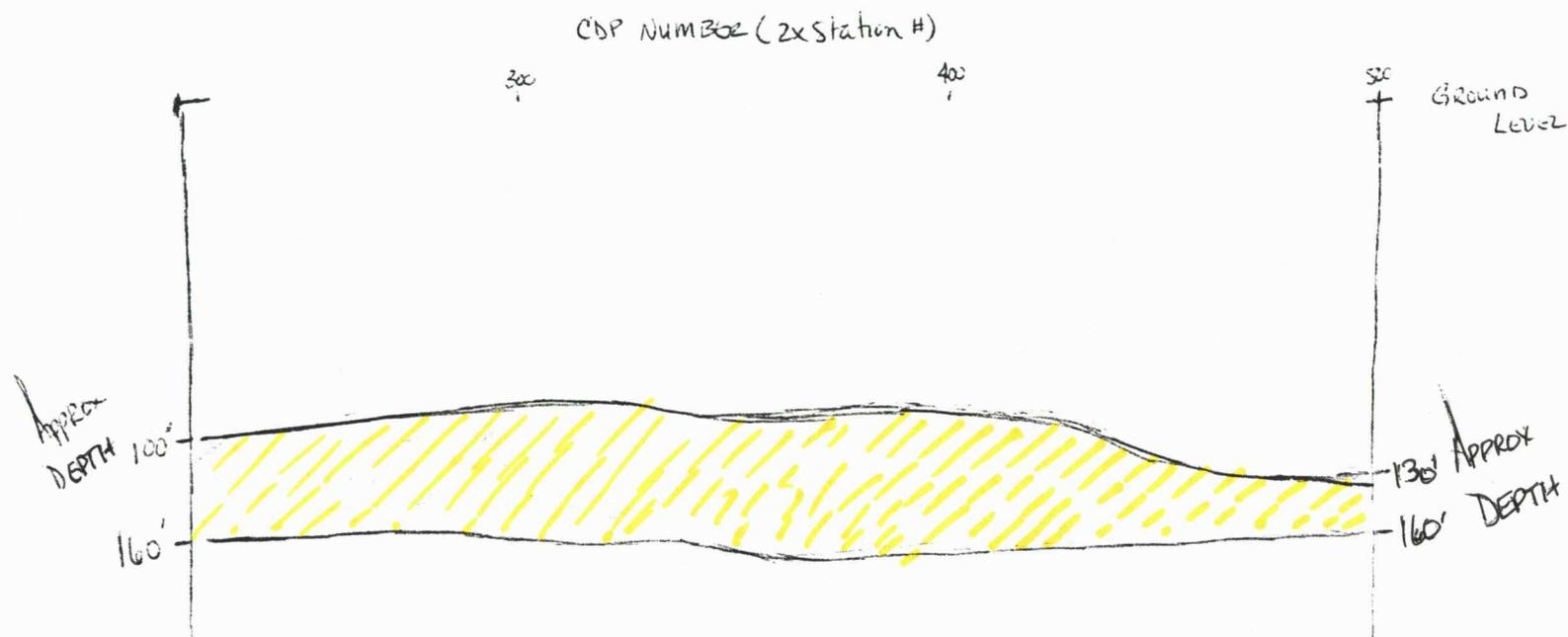Figure 26

CDP NUMBER (2x Station #)

V_{NMO} (100') depth = 2500 '/sec

V_{NMO} (160') depth = 2750 '/sec